THE ASTROPHYSICAL JOURNAL, 458:100–119, 1996 February 10

FAINT BLUE GALAXIES AND THE EPOCH OF DWARF GALAXY FORMATION

ARIF BABUL
Department of Physics, New York University, 4 Washington Place, New York, NY 10003; babul@alMuhit.physics.nyu.edu
AND
HENRY C. FERGUSON[1]
Space Telescope Science Institute, 3700 San Martin Drive, Baltimore, MD 21218; ferguson@stsci.edu
Received 1995 June 12; accepted 1995 August 17

ABSTRACT

Several independent lines of reasoning, both theoretical and observational, suggest that the very faint ($B \gtrsim 24$) galaxies seen in deep images of the sky are small low-mass galaxies that experienced a short starburst at redshifts $0.5 \lesssim z \lesssim 1$ and have since faded into low-luminosity, low surface brightness (LSB) objects. We examine this hypothesis in detail in order to determine whether a model incorporating such dwarfs can account for the observed wavelength-dependent number counts, as well as redshift, color, and size distributions.

Low-mass galaxies generically arise in large numbers in hierarchical clustering scenarios with realistic initial conditions. Generally, these galaxies are expected to form at high redshifts. Babul & Rees have argued that the formation epoch of these galaxies is, in fact, delayed until $z \lesssim 1$ due to the photoionization of the gas by the metagalactic UV radiation at high redshifts. We combine these two elements, along with simple heuristic assumptions regarding star formation histories and efficiency, to construct our bursting dwarf model. The slope and the normalization of the mass function of the dwarf galaxies are derived from the initial conditions and are not adjusted to fit the data. We further augment the model with a phenomenological prescription for the formation and evolution of the locally observed population of galaxies (E, S0, Sab, Sbc, and Sdm types). We use spectral synthesis and Monte Carlo methods to generate realistic model galaxy catalogs for comparison with observations. We find that for reasonable choices of the star formation histories for the dwarf galaxies, the model results are in very good agreement with the results of the deep galaxy surveys. Such a dwarf-dominated model is also qualitatively supported by recent studies of faint galaxy gravitational lensing and clustering, by galaxy size distributions measured with the *Hubble Space Telescope*, and by the evidence for very modest evolution in regular galaxy properties out to $z = 1$.

We also discuss various tests of the model based on some generic predictions. For example, the model predicts that the number counts in the K band ought to begin rising more steeply at magnitudes fainter than $K_{AB} \approx 24$–25. The model also predicts that the local field luminosity function (LF) ought to exhibit a steep upturn at magnitudes fainter than $M_B \approx -16$. The detection of the latter, however, depends sensitively on the selection criteria used to construct a galaxy catalog. We also consider the possibility of detecting the LSB remnants at low redshifts.

Subject headings: galaxies: formation — galaxies: luminosity function, mass function — galaxies: photometry

1. INTRODUCTION

The faint galaxies seen in deep images of the sky (see Koo 1986; Tyson 1988; Cowie et al. 1988) have been a source of great puzzlement since their detection. Data accumulated over the past decade suggest that the field galaxy population has undergone a dramatic evolution in the past 5–7 Gyr. In particular, the observations reveal a population of galaxies, first appearing at $B_{AB} \approx 23$ (Tyson 1988; Colless et al. 1993; Koo & Kron 1992), that have colors as blue as those of irregular galaxies today and, in some cases, significantly bluer than those of the bluest galaxies found locally, a tendency that is generally accepted as evidence for active star formation.[2] It is this faint blue population that we are most interested in.

As we discuss below, the observed properties of the faint blue galaxy population argue against them being directly associated with the known present-day population of galaxies and suggest that the faint blue galaxies represent a population of galaxies that become visible only while they experience a moderate starburst. Thereafter they simply vanish, principally by either merging with larger galaxies or fading. For this reason, we shall often refer to these faint blue galaxies as "boojums." (The word "boojums" is an acronym for "blue objects observed just undergoing moderate starburst" and has its origins in Lewis Carroll's poem "The Hunting of the Snark.")

The faint blue galaxies (or boojums) pose severe problems for standard models of galaxy evolution and cosmology. First, the total galaxy number-magnitude counts at the faint magnitudes greatly exceed the expectations of standard cosmological models ($0 < q_0 \leq 0.5$) containing only a nonevolving population of locally observed galaxies. As illustrated in Figure 1 of Lilly (1993), the galaxy counts are higher by a factor of 4–6 at $B_{AB} \approx 24$ and a factor of 6–8 higher at $B_{AB} \approx 27$ (see also Fig.

[1] Hubble Fellow.

[2] Most magnitudes in this paper are expressed in the AB system (Oke 1974), where $m = -2.5 \log f_\nu - 48.60$. Conversions to the Johnson system are $B = B_{AB} + 0.11$, $I = I_{AB} - 0.48$, and $K = K_{AB} - 1.8$. The wide B_J band used in many deep surveys is approximately $B_{AB} - 0.07$.

8). At the same time, the fraction of boojums rises rapidly toward increasingly fainter magnitudes to become a sizable, if not the dominant, fraction (Colless et al. 1993; Koo & Kron 1992).

Second, redshift surveys statistically complete to the limits attainable to date (that is, $B_{AB} \approx 24$ and $I_{AB} \approx 22.5$) reveal that the shape of the redshift distribution of faint galaxies is consistent with no-evolution expectations (Cowie, Songaila, & Hu 1991; Lilly 1993; Colless et al. 1993; Glazebrook et al. 1995); the median redshift of galaxies to $B_{AB} = 24$ is only $z \approx 0.4$ (Cowie et al. 1991; Glazebrook et al. 1995). For galaxies beyond the current limits of spectroscopy, the fact that the U-band observations of the boojums do not show evidence for the Lyman break having been redshifted through the passband (Guhathakurta, Tyson, & Majewski 1990) constrains the redshifts to be $z < 3$. More recently, gravitational lensing studies by Smail, Ellis, & Fitchett (1994) and Kneib et al. (1994) suggest that the bulk of the $B_{AB} \approx 26$–27 galaxies are neither low-z nor high-z galaxies, but, rather, they typically lie at redshifts $z \sim 1$.

Third, deep *Hubble Space Telescope* (*HST*) observations reveal that the boojums are very small (Mutz et al. 1994; Im et al. 1995). For a universe with $q_0 = 0.5$, the angular diameter–redshift relation turns over and $\theta(z)$ begin to increase beyond $z \approx 1.2$ (Sandage 1961). While the details are somewhat dependent on k-corrections and the galaxy mix, this feature becomes evident in the $\theta(m)$ relation at magnitudes well above the detection limits of *HST*. Comparison of predictions from standard no-evolution and passive-evolution models to the observed angular size distribution from the *HST* Medium Deep Survey (MDS) reveals a significant discrepancy (Im et al. 1995). Indeed, the angular sizes of galaxies continue to decrease with magnitude with roughly constant slope to the limits of the observations (see Fig. 2 of Griffiths et al. 1995). Such observations favor dwarf-dominated models over models involving passive evolution of the large, bright, locally observed galaxy population or a large population of low surface brightness (LSB) galaxies (Ferguson & McCaugh 1995).

Finally, the faint blue galaxies have been found to exhibit very weak clustering in comparison to the optically selected local bright galaxy population (Efstathiou et al. 1991; Neuschaefer, Windhorst, & Dressler 1991; Couch, Jurcevic, & Boyle 1993; Roche et al. 1993; Infante & Pritchet 1995; Brainerd, Smail, & Mould 1995). It is often suggested that the clustering of these objects may be comparable to that exhibited by present-day late-type galaxies, if one allows for evolution in the clustering. While this may be true for the brighter of the faint galaxies (that is, galaxies with $B_{AB} \lesssim 24$), studies such as that of Brainerd et al. (1995) show that the clustering properties of the boojums can only be reconciled with this suggestion if either their clustering evolved at an implausibly rapid rate or they are high-redshift galaxies. The above discussion about the redshift distribution of the faint blue galaxies argues against the latter possibility.

Early models of faint galaxy counts and redshift distributions started with the observed present-day galaxy mix and worked backward assuming constant comoving density of the galaxies, with evolution only in the stellar populations (e.g., Tinsley 1980; Yoshii & Takahara 1988; Koo 1990; Guiderdoni & Rocca-Volmerange 1990). In such models, most of the star formation occurs at relatively high redshifts ($z_f \gtrsim 5$), and recent evolution is mild, yielding a redshift distribution that is little different from the no-evolution case, with the exception of a high-redshift tail whose amplitude is extremely sensitive to assumptions about z_f, the star formation rate at high z, and the amount of dust mixed in with the stars during the starburst epoch. To match the observed optical counts, such models require the cosmology of the universe to be either open or Λ-dominated, so that there is sufficient volume out to intermediate redshifts to account for the large numbers of observed faint galaxies. For $q_0 \lesssim 0.2$, however, such models overpredict faint counts in the K band (Yoshii & Takahara 1988; Yoshii & Peterson 1995). Otherwise, such passive-evolution models successfully reproduce the color–apparent-magnitude trends, including the increase in the fraction of blue objects beyond $B_{AB} = 22$ (Koo 1990) and size-magnitude relations (at least to the limits of ground-based resolution). The most serious problem with such models is the rather robust prediction that many galaxies at and beyond $B = 24$ should have redshifts $z \gg 1$, which runs counter to most of the observations.

Gronwall & Koo (1995) have recently considered a variant of the passive-evolution model which starts with the colors, counts, and redshift distributions of faint galaxies and attempts to derive local color distributions and luminosity functions (LFs). With $q_0 = 0.05$, $H_0 = 50$, and $z_f = 5$, the model is reasonably successful and, in particular, shows good agreement with the redshift distributions and K-band counts, where standard passive-evolution models do not. Apart from the different approach to fitting the data, the two major departures of the model from previous passive-evolution models are (1) inclusion of dust in a way that is not tied to the chemical evolution of the galaxies (as it is, for example, in the models of Guiderdoni & Rocca-Volmerange 1990 or Wang 1991) and (2) the inclusion of a *nonevolving* population of very blue galaxies (their classes 1–3). To the extent that this latter population contributes to the counts, the model in a sense avoids discussing how the faint blue galaxies came to be and where they are at present. If the bluest classes of the Gronwall & Koo model really represent a starburst population, they must either leave a large population of faded remnants, not included in the model, or have a very high duty cycle of repeated bursts (in which case their colors would be different than assumed). In spite of this criticism, the Gronwall & Koo model is important in demonstrating that the problem of the high-redshift tail can perhaps be solved by a nonstandard treatment of dust in normal galaxies and the inclusion of a class of very blue, low-luminosity galaxies.

An alternative class of models does not conserve the comoving density of galaxies, but rather incorporates *wholesale* merging of the large number of faint galaxies seen at moderate redshifts into large galaxies at the present epoch (Guiderdoni & Rocca-Volmerange 1990, 1991; Broadhurst, Ellis, & Glazebrook 1992). In these models, the mass of a typical galaxy grows with time such that a typical L_* galaxy is approximately a factor of 2–3 less massive at redshift $z = 0.5$ and a factor of 3–5 less massive at $z = 1$. There are various problems with such scenarios. First, theoretical and N-body studies of realistic models for hierarchical structure formation (Lacey & Cole 1993; Kauffmann, White, & Guiderdoni 1993; Lacey & Cole 1994; Navarro, Frenk, & White 1994) show that high merger rates required by the above models are unlikely within the framework of a dynamical friction-driven merging scheme. Second, it is predicted that the present-day spiral galaxies in the heuristic *wholesale* merging models accreted as much as 40%–60% of their mass over the past 5 Gyr; Tóth & Ostriker (1992), however, argue that a typical spiral disk cannot have accreted more than 10% of its mass in the past 5 Gyr without

the disks being thicker than is observed. If the faint galaxies preferentially merged into the present-day elliptical galaxies, then there ought to be more blue light in the latter than is observed, unless the faint galaxies experienced rapid fading (Dalcanton 1993). If fading is invoked, then the merging hypothesis becomes superfluous, since fading itself can account for the steep decline in the galaxy counts. Third, if the boojums are declining in numbers due to wholesale mergers, one would expect that those at $B_{AB} \gtrsim 24$ ought to be at least as strongly clustered as the local population of bright galaxies. As discussed previously, most studies seem to indicate otherwise. (It should be noted that the clustering results do not argue against occasional mergers, only against *wholesale* mergers.) Finally and most importantly, observational studies of galaxies selected on the basis of their giving rise to Mg II absorption lines in spectra of background QSOs suggest that the present-day population of bright galaxies (both early-type and late-type) was already well established by $z \sim 1$ and has undergone no significant evolution since then in luminosity, color, size, or space density (Steidel & Dickinson 1994; Steidel, Dickinson, & Persson 1994). The authors are led to conclude that there must be "two distinct galaxy populations [present at $z \lesssim 1$], one of which must be evolving very rapidly while the other remains stable," and that "evolution of the faint blue galaxies apparently goes largely unnoticed by the [bright] galaxies."

Associating the boojums with a population of dwarf galaxies undergoing a short burst of star formation at moderate redshift that have since faded away is the basis of another class of models (Lacey & Silk 1991; Babul & Rees 1992; Gardner, Cowie, & Wainscoat 1993; Lacey et al. 1993; Kauffmann, Guiderdoni, & White 1994). The main differences among these models are the mechanisms for triggering and/or suppressing star formation in the dwarf galaxies. In the Lacey et al. (1993) model, the triggering mechanism is tidal interactions with normal galaxies. Kauffmann et al. (1994) propose no specific triggering mechanism, but their "bursting CDM" also assumes that dwarf galaxies only form stars in proximity to a larger galaxy. While the low-mass halos in such models are expected to be only weakly clustered (Efstathiou 1995), the fact that those that form stars are clustered much like regular galaxies leads to the expectation that the angular correlation function of boojums ought to be similar to that expected for the regular bright galaxies (if not even stronger if each bright galaxy has a cluster of bursting dwarfs in its vicinity). However, the observed correlation amplitude for the boojums is very small, suggesting that these galaxies are very weakly clustered (for example, see Brainerd et al. 1995). In the Babul & Rees (1992, hereafter BR92) model, on the other hand, the increase in the starburst activity in low-mass halos is correlated with the decline in the UV background in the universe, which enables the gas in the low-mass halos to cool, collapse, and undergo star formation. In this case, the likelihood of star formation in a given halo is not governed by the proximity of neighboring galaxies, although there may be some modulation by quasars and active galactic nuclei (AGNs) through the proximity effect.

In this paper we adopt the principal idea of the BR92 model, namely, that the boojums are dwarf galaxies whose formation has been delayed until $z \lesssim 1$ by photoionization. The mass function and size distribution of the dwarf galaxies are derived from fairly general considerations and are not adjusted to fit the data. An important feature of the model is that the number density of dwarf galaxy halos is *not* a free parameter. Hence the $N(m)$ and $N(z)$ relations for these dwarf galaxies depend only on their star formation histories and the selection functions of the surveys. Using Monte Carlo simulations of deep surveys, we show that with plausible choices for the star formation histories of the dwarf galaxies and their expansion during the supernova wind phase, as well as with a plausible model for the evolution of the locally observed population of galaxies (E, S0, Sab, Sbc, and Sdm types), we can achieve reasonable agreement with the observations. In subsequent papers, we will compare the models in detail to deep, high-resolution observations from *HST* (Ferguson, Giavalisco, & Babul 1995).

In § 2 of this paper, we outline and expand upon the BR92 model. In § 3, we describe our passive-evolution model for the locally observed population of galaxies, as well as the spectral-synthesis and the Monte Carlo methods used to simulate deep surveys. In § 4, we discuss the evolution of the individual galaxy types in our model and the evolution of the collective properties of the galaxy population. We compute, and compare with observations, the galaxy number counts as a function of magnitude in different bands, the redshift distribution, the LF (local), the color distribution, and the distribution of effective galaxy radii. The pros and cons of our model, and some possible tests, are discussed in § 5. Finally, we present a summary in § 6. Throughout this paper, we assume the $\Omega = 1$ Einstein–de Sitter model for the universe and adopt a Hubble constant of $H_0 = 50\, h_{50}$ km s^{-1} Mpc^{-1}.

2. BOOJUMS AS STARBURSTING DWARF GALAXIES

In keeping with the model outlined by BR92, we adopt the generally accepted hierarchical clustering scenario for galaxy formation as outlined by White & Rees (1978). In such scenarios, galaxies arise when density perturbations in a universe dominated by an unspecified type of dissipationless dark matter collapse under the action of gravity to form virialized dark halos, with star formation ensuing when the gaseous component of the halos cools and condenses in the central cores. The mass and the size (virial radius) of dark halos, in terms of redshift and the halos' circular velocity $V_c = (GM(R)/R)^{1/2}$, are

$$M = 7.5 \times 10^9\, h_{50}^{-1}\, V_{35}^3 \left(\frac{1+z}{2}\right)^{-3/2} M_\odot\,, \tag{1}$$

where $V_{35} = V_c/35$ km s^{-1} and

$$R = 13.3\, h_{50}^{-2/3} \left(\frac{M}{10^9\, M_\odot}\right)^{1/3} \left(\frac{1+z}{2}\right)^{-1} \text{kpc}\,. \tag{2}$$

For simplicity, we assume that the virialized dark halos have spherically symmetric density profiles

$$\rho(r) \propto 1/(r^2 + r_c^2)\,, \tag{3}$$

where r_c is a core radius. In the absence of any natural length scale for the core radius, we assume that $r_c \propto R$ and, more specifically,

$$r_c = 1.0\, h_{50}^{-2/3} \left(\frac{M}{10^9\, M_\odot}\right)^{1/3} \left(\frac{1+z}{2}\right)^{-1} \text{kpc}\,. \tag{4}$$

It should be noted that our adopted value for the core size is not inappropriate; local gas-rich dwarf galaxies, whose rotation curves have been well studied and which appear to be almost completely dominated by dark matter, have density profiles that can be approximated as isothermal spheres with

core radii of order 3–7 kpc (see Moore 1994 and references therein).

BR92 associate the faint blue galaxies with minihalos having $15 \lesssim V_c \lesssim 35$ km s^{-1}. In generic hierarchical models for galaxy formation, such minihalos should condense from the expanding background and virialize at high redshifts. For example, in the standard $\Omega = 1$ cold dark matter (CDM) model for structure formation with a power spectrum normalized such that the rms density fluctuation in a sphere of radius $16\ h_{50}^{-1}$ Mpc is $\sigma_8 = 0.67$, the bulk of $M \sim 10^9\ M_\odot$ halos virialize at $z \approx 3.5$. Ordinarily, one would expect that the minihalos would experience a starburst soon after virialization. However, observations of Lyα clouds at high redshifts suggest that, at these redshifts, the universe is permeated by a metagalactic UV flux originating in quasars and young galaxies. At $z = 2$, this background is estimated to have a strength $J_\nu \approx 10^{-21}$ ergs cm^{-2} s^{-1} Hz^{-1} at the Lyman limit (Bechtold et al. 1987). Such an ionizing flux is intense enough to photoionize the gas in collapsing minihalos and maintain it at a temperature of $T \approx 3 \times 10^4$ K. In dark halos with 15 km s$^{-1} \lesssim V_c \lesssim 35$ km s^{-1}, the photoionized gas would be stably confined, neither able to escape nor able to settle to the center (Rees 1986; Ikeuchi 1986), until the intensity of the metagalactic ionizing flux declines sufficiently.

Although the epoch dependence of the UV flux is uncertain at higher redshifts, it seems almost certain that at smaller redshifts J_ν is a steeply declining function of z. The sources of the UV background, whether they be quasars or young galaxies, are likely to be less intense per comoving volume at low redshifts. In the absence of any sources at $z < 2$, J_ν would scale as $(1 + z)^{3+\alpha}$, where α is the spectral index. A more detailed analysis by Zuo & Phinney (1993) suggests that the J_ν declines as $(1 + z)^3$.

A declining J_ν has two effects on the gravitationally bound gas cloud in the minihalos. First, the equilibrium temperature of the highly photoionized gas depends, albeit somewhat weakly, on J_ν (see Black 1981), and this would cause a gradual concentration toward the center (Ikeuchi, Murakami, & Rees 1989). Second, the gas becomes more neutral and offers a greater optical depth to the ionizing photons, leading to a diminution of the ionizing flux reaching the central regions and the formation of a warm ($T \approx 9000$ K) shielded neutral core (Murakami & Ikeuchi 1990) in pressure equilibrium with an ionized envelope. The formation of a neutral core, however, is not a sufficient condition for star formation to ensue. For a gas cloud to be susceptible to star formation, it must be at least marginally self-gravitating (e.g., Matthews 1972). To satisfy this constraint, the entire baryonic component of a minihalo must accumulate within a central region of size

$$R_b \approx 1.9\ h_{50}^{-2/3} \left(\frac{M}{10^9\ M_\odot}\right)^{1/3} \left(\frac{1+z}{2}\right)^{-1} \text{kpc}\ , \qquad (5)$$

if $\Omega_b = 0.1$, and this can occur only if the gas in the neutral core can cool below 9000 K.

Further cooling of a neutral metal-poor gas is only possible if H_2 molecules form. The formation of molecular hydrogen in a gas of primordial composition occurs via gas-phase reactions (see Shapiro & Kang 1987). In the presence of ionizing radiation, molecular hydrogen will not form efficiently until the region in question is effectively shielded against photons with energies greater than 25 eV that photoionize helium (Kang et al. 1990). BR92 have argued that the rapid decline in the intensity of the background UV flux at $z < 2$, coupled with the increasing efficiency in shielding of the central regions, will give rise to appropriate conditions for the formation of molecular hydrogen at $z \sim 1$ (see also Babul & Rees 1993). Thereafter, the temperature of the gas in the core plummets down to $\sim 10^2$ K. With the resulting loss of pressure support from the core, the baryons in the ionized envelope will also collapse (the phenomenon is analogous to that studied by Shu 1977) and accumulate at the center of the potential well.

The foregoing argument suggests that most of the low-mass halos, despite having virialized early, would experience a long "latency" period before forming stars. During this period, some of the stable minihalos may merge and become incorporated into larger systems (and therefore no longer be stable minihalos), while new minihalos may condense out of the general background. In hierarchical clustering scenarios with realistic initial conditions on galactic and subgalactic scales (i.e., spectral index $-2 \lesssim n \lesssim -1$), the distribution of low-mass halos is a steep function of mass ($d \ln N / d \ln M \approx -2$). For example, assuming that the power spectrum of density fluctuations that grow into halos of interest is adequately described by the standard CDM power spectrum normalized such that $\sigma_8 = 0.67$, that is,

$$\sigma(M) = 7.5 \left(\frac{M}{10^9\ M_\odot}\right)^{-0.1}\ , \qquad (6)$$

the comoving number density of minihalos existing at $z \approx 1$ estimated using the analytic Press-Schechter formalism (Press & Schechter 1974) is

$$\frac{dN}{d \ln M} \approx 2.3 \left(\frac{M}{10^9\ M_\odot}\right)^{-0.9} \text{Mpc}^{-3}\ . \qquad (7)$$

According to Lacey & Cole (1993), minihalos existing at $z \approx 1$ have long survival times. Almost all of the minihalos existing at $z \approx 1$ will survive for roughly 5 Gyr, and up to 40% will survive to the present.

As originally noted by BR92, the actual redshift at which the UV background ceases to be able to prevent baryonic collapse (and the subsequent star formation activity) in a particular minihalo depends sensitively on its particular density profile.[3] It is not possible at present to make a detailed prediction of the redshift range over which this baryonic collapse occurs or its dependence on galaxy mass. For present purposes, we assume that the probability that a given halo will experience starburst at some Hubble time t is described by an exponential decay:

$$p(t)dt \propto e^{-t/t_*}\ dt\ , \qquad (8)$$

where t_* is the exponential decay timescale, the formation timescale for the dwarf population as a whole. We further assume that no halo will experience a starburst at redshifts $z > 1$. With such a burst probability, we can, by varying the value of t_*, explore the consequences of having a nearly constant probability from $z = 1$ to the present (large values of t_*)

[3] Chiba & Nath (1994) argue that the decline in J_ν at low redshifts is unlikely to trigger the formation of low-mass galaxies. However, we believe this is a result of their using top-hat density profiles for low-mass halos. Consider two objects of the same size R and mass $M = 4\pi\rho_0 R^3$, one being a singular sphere with density profile $\rho(r) = \rho_0 (R/r)^2$ and the other a uniform sphere with $\rho(r) = 3\rho_0$. The column density (optical depth) through the center is finite for one and infinite for the other. A top-hat model is the limiting case of a density profile that would be *least* able to cool in the presence of metagalactic ionizing background radiation.

or the consequences of having all the halos bursting at redshifts close to unity (small values of t_*).

Within an individual halo, the natural scaling for star formation rate in a self-gravitating gas cloud is

$$\dot{M}_* \propto \frac{M_g(t)}{t_{\rm ff}}, \tag{9}$$

where $M_g(t)$ is the instantaneous mass of gas cloud and $t_{\rm ff}$ is the free-fall timescale for the cloud. As noted by BR92, the duration of the starburst in minihalos is expected to be relatively short ($\tau_{\rm SB} \approx 10^7$ yr); the very first generation of supernovae will expel all the gas out of the dwarf galaxy, quenching further star formation (see also Larson 1974; Dekel & Silk 1986). We therefore assume that during starburst, the star formation rate is constant and equal to the initial value.

For a gas cloud of mass $M_g = \Omega_b M$ and radius R_b at the center of a minihalo of mass $M \sim 10^9\ M_\odot$, the star formation rate is of order unity and is proportional to mass. We express the star formation rate as

$$\dot{M}_* = \epsilon_* \frac{M}{\tau_{\rm SB}} = 100\epsilon_* \left(\frac{M}{10^9\ M_\odot}\right)\left(\frac{\tau_{\rm SB}}{10^7\ {\rm yr}}\right)^{-1} M_\odot\ {\rm yr}^{-1}, \tag{10}$$

where $0 < \epsilon_* \leq \Omega_b$ is the fraction of the *total* halo mass that is converted into stars by the end of the starburst. In effect, ϵ_* represents the star formation efficiency and characterizes our ignorance regarding details of the supernova heating of the interstellar medium and of the mass loss.

In a starburst galaxy, the flux at wavelengths shortward of the Balmer discontinuity is dominated by massive young stars and, therefore, the UV luminosity of the galaxy is primarily determined by the instantaneous star formation rate (White & Frenk 1991). Furthermore, the observed B-band flux from a galaxy lying in the redshift range $0.3 < z < 3$ is a direct measure of this luminosity. Consequently, a galaxy at redshift z with a star formation rate $\dot{M}_*$ will be observed to have a B-band magnitude

$$B_{\rm AB} = -13.17 - 2.5 \log (l_B/1\ {\rm ergs\ s^{-1}\ cm^{-2}}), \tag{11}$$

where

$$l_B = L_{\rm UV}(\dot{M}_*/1\ M_\odot\ {\rm yr}^{-1})\Delta\nu(1+z)/4\pi d_L^2, \tag{12}$$

$\Delta\nu = 1.6 \times 10^{14}$ Hz is the effective bandwidth, $d_L = 1.2 \times 10^4\ h_{50}^{-1}(1+z)[1-(1+z)^{-1/2}]$ Mpc is the luminosity distance, and $L_{\rm UV} \approx 6.7 \times 10^{26}$ ergs s^{-1} Hz^{-1} is the UV luminosity of the star-forming region assuming a Salpeter initial mass function (IMF) truncated at 0.1 and 100 $M_\odot$. A galaxy of mass 10^9 $M_\odot$ that converts 3% of its total mass (30% of its baryonic mass if $\Omega_b = 0.1$) into stars during a $\tau_{\rm SB} = 10^7$ yr burst at $z = 0.4$ would have an apparent magnitude of $B_{\rm AB} \approx 24.9$. At $z = 1$, the same galaxy would have an apparent magnitude of $B_{\rm AB} \approx 26.7$. For a fixed value of ϵ_*, the contribution of the dwarfs to faint galaxy counts is clearly sensitive to the duration of the starburst. If the star formation timescale were more than a few times 10^7 yr, the dwarfs would not be bright enough to contribute to the counts near $z = 1$. On the other hand, very short burst phases would produce too many galaxies brighter than $B = 24$, unless the star formation efficiency were much lower as well. Thus, in order to dominate the faint galaxy counts, the dwarfs at $z \approx 1$ must form stars within a timescale that fortuitously turns out to be roughly that expected if supernovae terminate the starburst.

The expulsion of the gas from the galaxy, and the resulting reduced gravity, cause the remnant stellar system to expand. The degree of expansion, however, is moderated by the presence of the dark halo. If the timescale for mass loss is longer than the dynamical timescale in the central star-forming region, the stars in the galaxy respond adiabatically to the mass loss. The radii of the orbits before and after the mass are related by $r_i M_i(r_i) \approx r_f M_f(r_f)$, where $M(r)$ is the total mass (baryons + dark matter) within radius r, and the subscripts i and f refer to the initial and final states, respectively (Dekel & Silk 1986; Lacey et al. 1993). In a galaxy that converts 30% of its baryons ($\Omega_b = 0.1$) into stars and expels the rest, the stellar system will expand by a factor of 1.3. The degree of expansion under the assumption that the mass loss occurs instantaneously is comparable.

The key assumption of our model is that star formation occurs in bursts. If star formation in the low-mass halos predicted by CDM is quiescent, extending over more than a few times 10^7 yr, then these galaxies will never be bright enough to influence the faint galaxy counts. There is ample evidence from studies of nearby dwarf galaxies that star formation does occur in bursts, and that galactic winds play a key role in influencing the star formation histories (e.g., Searle, Sargent, & Bagnuolo 1973; Meurer et al. 1992; Marlowe et al. 1995; Armus et al. 1995; Tosi 1993). Nevertheless, the model described above is clearly a vast oversimplification of the real world. In general, dwarf galaxies will not be spherical, will not all have the same density profile, will not have a step-function star formation hsitory, and will not expel all their remaining gas at the end of the starburst. Furthermore, the stellar populations (described in § 3) undoubtedly will not all have the same IMF and metallicity. An ideal physical model would predict the distribution functions of all of these parameters and integrate over the population to compare to deep survey observations. However, this is well beyond current capabilities. Instead, we assume that in a broad statistical sense all of these details can be subsumed in the parameters t_*, which governs the probability distribution of star formation episodes as a function of redshift, and ϵ_*, which governs the luminosity released in an average star formation episode. Thus, the simplifying assumption of a single burst of star formation followed by ejection of all the remaining gas is not essential to our model, as long as the star formation occurs in episodes with a relatively high star formation rate (1–10 $M_\odot$ yr^{-1}) and with an overall time evolution of the burst probability similar to our assumed exponential law. The essential features of our model (see § 4)—that the population at $B > 25$ is primarily low-mass galaxies at $z < 1$, that the population is weakly clustered, and that the remnant population still exists at present as LSB dwarfs—are largely independent of the details of the starbursts within the individual galaxies.

3. TESTING THE BURSTING DWARF HYPOTHESIS

The simplest and most efficient way of comparing the model to observations is through the analysis of model galaxy catalogs, generated by Monte Carlo methods, that incorporate the appropriate survey selection criteria and magnitude estimation schemes. The Babul-Rees (or the "boojums as bursting dwarfs") hypothesis, in and of itself, only specifies the formation and evolution of low-mass "dwarf" galaxies. In order to generate realistic galaxy catalogs for comparison with observations, we combine the fading dwarfs model with a prescription for the formation and evolution of the locally observed population of galaxies. We divide the latter population into five

galaxy types: E, S0, Sab, Sbc, and Sdm. Thus our model is a hybrid approach that works forward from initial conditions for the dwarfs, but works backward from present-day properties for the "normal" galaxies. The rationale for this approach is that the star formation histories along the traditional Hubble sequence are reasonably well constrained from observations of nearby galaxies, but not very well constrained from hierarchical structure models. On the other hand, the steep mass function of the dwarf galaxies is a *robust* consequence of a hierarchical structure built from CDM-like power spectra, even if such low-mass galaxies are not well represented in the *observed* local LF.

The procedures for creating the model catalogs can be summarized as follows: Galaxy candidates and their internal properties are drawn at random from distribution functions for galaxy type, total luminosity, bulge/total mass ratio (our galaxies are made up of bulges and disks whose stellar populations and luminosity profiles are modeled separately), surface brightness, redshift, and age. For each galaxy considered, we follow the evolution of its stellar population to the required age and compute the associated synthetic spectrum. The galaxy is then "observed" and included in the catalog if it conforms with the selection criteria. These steps and our specific assumptions are described in more detail in the following subsections.

3.1. *Evolution of the Stellar Population*

3.1.1. *Model Inputs*

In order to compute the synthetic spectra of each galaxy under consideration, it is necessary to trace the evolution of its stellar population as a function of the galaxy's age. Stellar evolution theory provides us with the effective temperature $T_{\rm eff}(M, Z, t)$ and bolometric luminosity $L_{\rm bol}(M, Z, t)$ of a star of mass M and metallicity Z as a function of time. Ignoring chemical evolution, one can determine the stellar population of a galaxy given a complete set of $L_{\rm bol}$ and $T_{\rm eff}$ evolutionary tracks as well as the IMF $\phi(M)$, which specifies the number of stars of mass M born per unit mass when a stellar population is born, and the star formation rate $\Psi(t)$. To compute accurate spectra at early times requires interpolation between evolutionary tracks for stars of different masses, a procedure that is equivalent to computing isochrones. Rather than start with the evolutionary tracks, therefore, it is more convenient to begin with isochrones which give $L_{\rm bol}$, $T_{\rm eff}$ on a fine grid of M, t, as advocated by Charlot & Bruzual (1991) and Bruzual & Charlot (1993).

Due to the paucity of theoretical models covering all phases of stellar evolution, Charlot & Bruzual (1991) were forced to piece together isochrones from a variety of theoretical evolutionary tracks and empirical sources (for asymptotic giant branch [AGB] stars). Since the Bruzual & Charlot (1993) models, new isochrones have become available that cover a wider range of stellar masses and phases of evolution in a self-consistent manner (Bertelli et al. 1994). Hence, we avoid some of the difficulties encountered by Charlot & Bruzual (1991) in trying to merge tracks computed by different authors with different sets of opacities. The new isochrones have been used for spectral synthesis by Bressan, Chiosi, & Fagotto (1994), to which the reader is referred for a summary of the basic physical assumptions underlying the stellar evolution models. Our galaxy models are constructed from stellar populations of a single metallicity. For E, S0, Sab, Sbc, and Sdm galaxies, we use $Z = 0.02$ (i.e., $Z = Z_\odot$) for both the bulge and the disk stars. For the dwarfs, we use $Z = 0.001$ ($Z = Z_\odot/20$; [Fe/H] $= -1.3$). One of the advantages of the Bertelli et al. isochrones is that these isochrones cover a wide range of metallicities: $Z = 0.0004$, 0.001, 0.004, 0.008, 0.02, and 0.05, with corresponding helium abundances $Y = 0.23$, 0.23, 0.24, 0.25, 0.28, and 0.352. We are therefore in a position to construct more realistic spectra for low-metallicity galaxies than previously possible for models of faint galaxy counts.

We adopt an exponential star formation law for the bulges and disks of the nondwarf galaxies, and tune their star formation histories so that their present-day colors (for the total bulge + disk light) match "standard" colors of the local galaxies. Table 1 shows the adopted colors and the corresponding e-holding timescales for star formation in the bulges and disks of the different galaxy types. For the dwarfs, we assume a starburst with a constant star formation rate over 1×10^7 yr. Thereafter, the galaxy undergoes pure passive evolution (no star formation).

3.1.2. *Computing Model Spectra*

We begin by assuming that stars form according to the Salpeter IMF, $dN/dM \propto M^{-2.35}$, with lower and upper mass limits of 0.1 and 100 $M_\odot$. Using the isochrone synthesis algorithm, we derive theoretical values for the bolometric luminosity $L_{\rm bol}$ and effective temperature $T_{\rm eff}$ of the stars in a population as a function of initial mass and age. For each group of stars of a given initial mass and age, we next search our catalog of synthetic stellar spectra (based entirely on model atmospheres of Kurucz 1992 for $T_{\rm eff} < 5000$ K and of Clegg & Middlemass 1987 for 5000 K $< T_{\rm eff} <$ 200,000 K) for the nearest match in $T_{\rm eff}$ and then (at fixed $T_{\rm eff}$) in log g. The gravity of a star is

$$\log g = \log (M/M_\odot) + 4 \log T_{\rm eff} - \log (L/L_\odot) - 10.604 , \tag{13}$$

where M is the *current* mass of the star, taking into account the mass lost in all previous stages of evolution, as tabulated by Bertelli et al. (1994).

The spectrum of the galaxy is the weighted sum of the different model atmosphere spectra. The weight accorded to the flux from each model atmosphere is

$$w = 4\pi r^2 T_c\, g_c\, \phi(M) dM\, \Psi(t) dt , \tag{14}$$

where

$$r = \sqrt{GM/g} \tag{15}$$

is the radius of the star, the IMF $\phi(M)$ specifies the fraction of the total number of stars formed at any given time with masses in the range M to $M + dM$, and the star formation rate $\Psi(t)$ specifies the fraction of the population being a particular age. The remaining factor ($T_c\, g_c$), where

$$T_c = T_{\rm eff}^4/T_{\rm eff}^4({\rm grid}) \quad \text{and} \quad g_c = g({\rm grid})/g , \tag{16}$$

corrects for the mismatch between the actual temperatures and gravities of the stars, and those available in the grid. The factor ensures that the bolometric flux is correct even though the detailed spectral shape may be slightly off due to the finite $T_{\rm eff}$, log g sampling of the model atmosphere grid.

Our model spectra do not include emission lines from H II regions or supernova remnants, but they do include extinction

TABLE 1

GIANT GALAXY COLORS AND STAR FORMATION TIMESCALES

		Observed Means			Model Colors			e-Folding Times	
Type	Bulge/Total	$U-B$[a]	$B-V$[a]	B_J-K[b]	$U-B$	$B-V$	B_J-K	Bulge	Disk
E	1.0	0.54	0.96	3.91	0.61	1.07	3.90	0.01	...
S0	0.4	0.54	0.96	3.91	0.61	1.07	3.90	0.01	1.0
Sab	0.3	0.10	0.79	3.08	0.12	0.73	3.36	0.01	30.0
Sbc.....	0.15	−0.09	0.64	3.06	−0.01	0.63	3.21	0.01	30.0
Sdm.....	0.0	−0.15	0.54	3.06	−0.14	0.50	2.83	...	30.0

[a] From Tinsley 1978.
[b] From Mobasher, Ellis, & Sharples 1986.

due to dust during the rapid star formation phase of giant galaxies. The addition of dust is motivated by the success of the models of Wang (1991) and Gronwall & Koo (1995) in removing the high-redshift tail from standard passive-evolution models. While the amount of dust and the shape of the extinction curve, in principle, must depend on chemical evolution, in practice there is only a weak dependence on metallicity seen in the dust properties of nearby starburst galaxies (Calzetti, Kinney, & Storchi-Bergmann 1994; Storchi-Bergmann, Calzetti, & Kinney 1994). The form of the extinction probably depends mostly on how the stars and dust are mixed together.

We have included dust in our models only during the rapid formation phases of ellipticals, bulges, and S0 disks. Dust will *inevitably* accompany star formation in such systems, but modeling its detailed evolution is beyond the scope of this paper. For our purposes, we have simply adopted the "extinction curve" of Calzetti et al. (1994), with τ_B varying smoothly from zero at the birth of the galaxy to $\tau_B = 1$ at the peak of the star formation epoch, falling to $\tau_B = 0$ again by late epochs, as shown in Figure 1. While the model is ad hoc, these optical depths are probably underestimates. Nevertheless, they are sufficient to remove high-redshift galaxies from samples down to $B = 24$. For our purposes, then, the details of the dust evolution do not matter so long as the attenuation is $\tau_B \gtrsim 1$ during the starburst phase. Spectra of E and S0 galaxies have been set to zero beyond the Lyman limit.

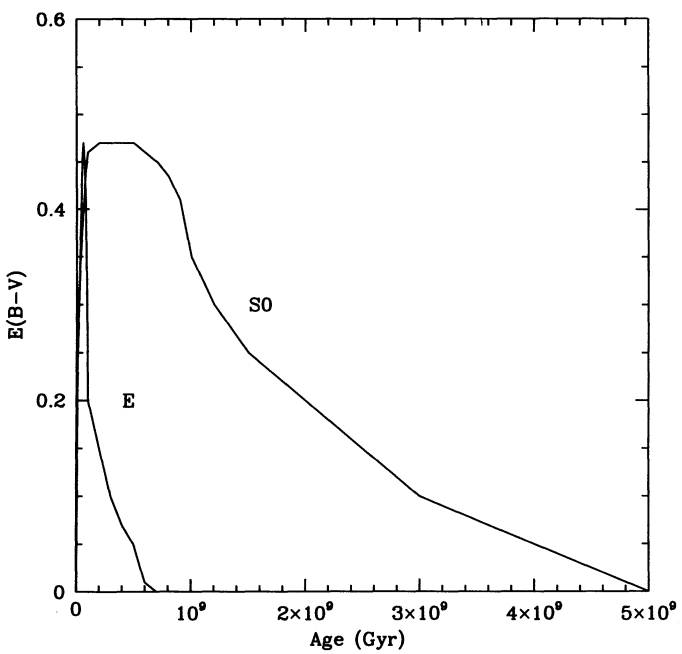

FIG. 1.—Evolution of interstellar reddening assumed for bulges and ellipticals (E) and for S0 galaxy disks.

3.1.3. *Uncertainties in the Models*

It is well known that synthetic spectra from model atmospheres do not provide a perfect match to real stellar spectra. The most serious discrepancies arise at the extremes of the temperature and gravity ranges sampled by the model atmosphere grids. At low temperatures, molecular opacity becomes important but is not fully included in the model atmospheres. At high temperatures and low gravities, non-LTE effects become important.

A standard procedure for circumventing these difficulties is to use empirical spectra of individual stars, especially at cool temperatures. This is the technique adopted, at least in part, by Bruzual & Charlot (1993) and Bressan et al. (1994). For simplicity and expediency, we have chosen to rely entirely on model atmospheres, recognizing that this may cause problems at some ages and wavelengths. The biggest drawback of this approach is the lack of theoretical synthetic spectra for stars cooler than $T_{\rm eff} = 3500$ K. We associate such stars with the coolest Kurucz model atmosphere. Our procedure for computing the model atmosphere weights ensures that the total bolometric luminosity of the star will be correct; however, the flux will be distributed differently from the overall spectral energy distribution of a real M star.

We can estimate the uncertainties associated with our procedure for computing model galaxy spectra by comparing spectra for simple, single-metallicity coeval stellar populations (SSPs) to those computed by Bressan et al. (1994). The spectra are constructed from the same underlying isochrones, although by different codes. However, Bressan et al. (1994) supplemented the Kurucz model grid with observed spectra of stars cooler than $T_{\rm eff} = 3500$ K. Figure 2 shows the comparison for a solar metallicity SSP at ages 10^7, 10^8, 10^9, and 10^{10} yr. The differences between the spectra are minor, typically a few hundredths of a magnitude. Figure 3 shows the same comparison for a population of $0.02\ Z_\odot$. Once again, the difference introduced by our reliance on model atmospheres are very minor.

More serious differences are introduced by the use of different theoretical isochrones. The dashed curves in Figure 2 show SSP spectra computed using the Bruzual & Charlot (1993) code, which relies on a different set of underlying isochrones (e.g., based on the evolutionary tracks of Schaller et al. 1992 for massive stars). The differences in colors computed from our synthetic spectra and those of Bruzual & Charlot can be up to ~ 1 mag in rest-frame $B-K$, but are typically much smaller (see also Charlot, Worthey, & Bressan 1996).

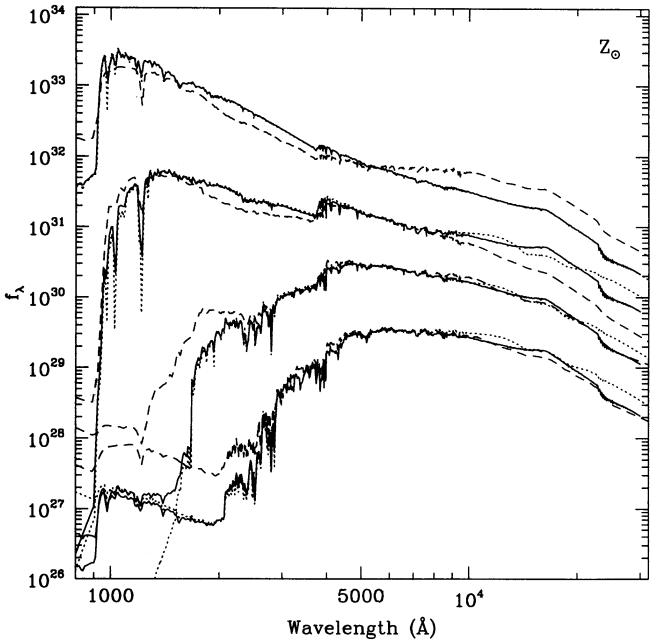

FIG. 2.—Comparison of spectral energy distributions for simple stellar populations of composition $Z = 0.02$, $Y = 0.28$, and ages 10^7, 10^8, 10^9, and 10^{10} yr. Solid curves show the spectra used in this paper constructed from the Bertelli et al. (1994) isochrones and model atmospheres as described in the text. Dotted curves show spectra constructed from the same isochrones by Bressan and coworkers (A. Bressan 1995, private communication) using both model atmospheres and empirical stellar spectra as described in Bressan et al. (1994). Dashed curves show synthetic spectra from the Bruzual & Charlot (1993) code, which uses a different set of isochrones and a different library of stellar spectra.

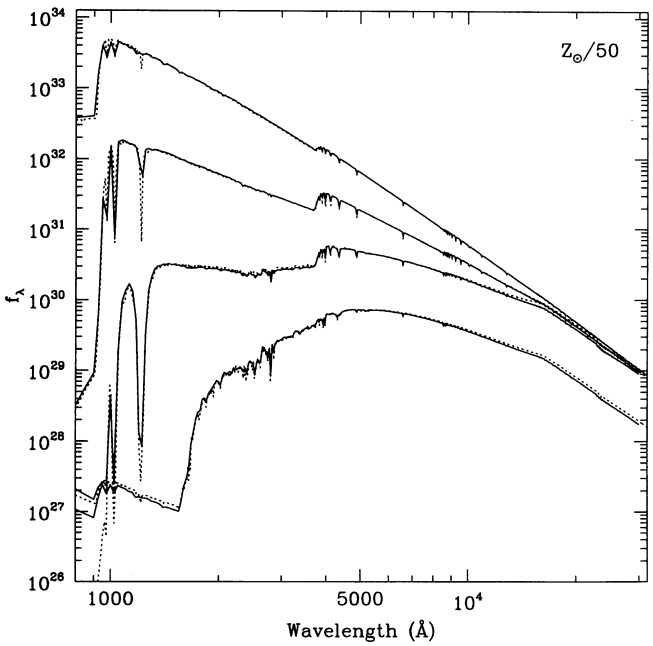

FIG. 3.—Comparison of spectral energy distributions for simple stellar populations with $Z = 0.0004$, $Y = 0.23$ for ages 10^7, 10^8, 10^9, and 10^{10} yr. Solid curves show the spectra used in this paper constructed from the Bertelli et al. (1994) isochrones and model atmospheres as described in the text. The Kurucz atmospheres used here are for [Fe/H] = −1.5. Dotted curves show spectra constructed from the same isochrones by Bressan and coworkers. (A. Bressan 1995, private communication) using both model atmospheres (interpolating in metallicity) and empirical stellar spectra (for solar metallicity) as described in Bressan et al. (1994). The agreement indicates that the model spectral energy distributions are relatively insensitive to the different techniques for assigning stellar spectra to the isochrone points.

Since our models are based entirely on theoretical isochrones and theoretical model atmospheres, it is quite simple to investigate the effects of varying the chemical composition. Figure 4 shows our computed spectra for metallicities $Z_\odot$ and $Z_\odot/50$. Changing metallicities introduces differences of up to 3 mag in rest-frame $B-K$ colors at fixed age. *These differences are almost entirely due to differences in the isochrones*; model spectra constructed using low-metallicity ($Z_\odot/50$) isochrones and solar-metallicity atmospheres differ by at most a few tenths of a magnitude from the curves shown in Figure 4.

We now summarize and rank the importance of the errors introduced by our various approximations. For computing counts and redshift distribution, the most important and least constrained aspect of the model is the early photometric evolution of early-type galaxies and spiral-galaxy bulges. As outlined above, our assumptions for the photometric evolution and, in particular, the amount of dust during the star formation epoch in these galaxies were motivated by the need to remove the high-z tail from the redshift distribution. The star formation rates and the amount of dust needed to do this are entirely plausible. Of course there are other ways to remove the high-redshift tail (e.g., by forming all bulges and early-type galaxies at low redshift), but we find the local evidence that stars in these systems are mostly old is too compelling to adopt this point of view.

Next in importance is any potential mismatch between the metallicity assumed in our models and those of real galaxies. Our assumption of a single metallicity is a vast oversimplification, but it is difficult to overcome without constructing a chemical evolution model for each galaxy type. Generally, we expect that the normal galaxies will be bluer at early epochs

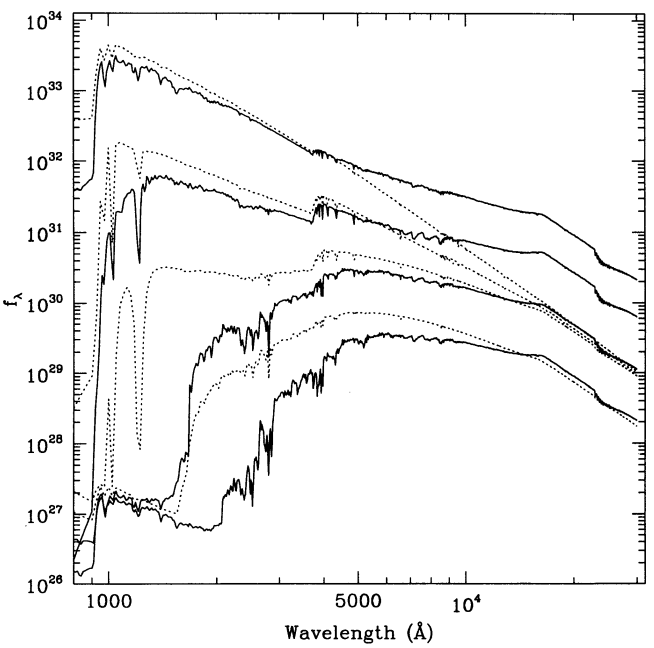

FIG. 4.—Comparison of spectral energy distributions for simple stellar populations with $Z_\odot$ (*solid curves*) and $Z_\odot/50$ (*dotted curves*) for ages 10^7, 10^8, 10^9, and 10^{10} yr. Our dwarf galaxy spectra are calculated to assume $Z_\odot/20$ and, hence, are intermediate between the two extremes shown here.

than we have assumed. In the case of the dwarf galaxies, our choice of metallicity may have some effect on optical-infrared colors. We do not expect that adding more realistic chemical evolution would significantly alter the predicted counts or redshift distributions, because these are primarily determined by the assumptions for the star formation rate versus time and the initial mass function.

Modifications of the *slope* of the IMF are likely to have a very small effect on the slope of the number counts or the median of the redshift distribution (Kauffman et al. 1994). Modifications in the upper and lower mass limits of the IMF do affect the counts but essentially trade off against the star formation efficiency ϵ_*. If the lower-mass limit were raised from 0.1 to 0.5 $M_\odot$, the required star formation efficiency would be significantly lower. Uncertainties in the underlying stellar isochrones probably have a negligible effect on the optical counts and colors but may influence the K-band counts and optical-infrared colors at a level of up to a magnitude. Finally, the adoption of model atmospheres for cool stars instead of empirical stellar spectra probably does not introduce any significant errors in any of the faint galaxy distribution functions.

3.2. *Distribution Functions for Locally Observed Galaxies*

Apart from being able to follow the spectral evolution of galaxies, we need to specify the mass functions, bulge/disk ratios, and surface brightness distributions for the different galaxy types in order to generate realistic galaxy catalogs.

For the locally observed galaxy population, we normalize the spectra so that galaxies with fiducial "mass" $M_0 = 1.0$ have $M_{B_J} = -21.1$ at an age of 1.3×10^{10} yr. All LFs are then specified in terms of fiducial mass. This automatically corrects for any mismatch between our adopted mass limits for the IMF and the true ones in galaxies.

The LFs for the different galaxy types are Gaussian, with parameters chosen so that the individual LFs approximate those shown in Binggeli, Sandage, & Tammann (1988), while the overall LF has a Schechter (1976) function profile over the range $M_{B_J} = -23$ to -16, with ϕ_* set to 2.3×10^{-3} galaxies Mpc^{-3} (Yoshii & Takahara 1988). We note that this assumed LF for the locally observed, "normal" population of galaxies has a pronounced deficit of galaxies fainter than $M_{B_J} \approx -15$, which will be filled in by the brighter members of the faded dwarf population.

The Gaussian approximation for the LFs of individual galaxy types implies that the fiducial mass of a given galaxy of a particular type in the Monte Carlo simulation can be assigned according to

$$M_0 = 10^{\log \langle M_0 \rangle - 0.4\sigma g}, \tag{17}$$

where g is a Gaussian random deviate with unit variance. The parameters $\langle M_0 \rangle$ and σ, the mean and the dispersion of the mass functions, are listed in Table 2. In addition, this table also lists the local space density in galaxies per cubic megaparsec, integrated over the mass function from a lower limit of $3.5 \times 10^{-3} \langle M_0 \rangle$ to an upper limit of $10 \langle M_0 \rangle$.

Table 2 also lists our adopted mean bulge-to-total light ratios (B/T) and scatter, taken from Simien & de Vaucouleurs (1986), for the different galaxy types. For a given galaxy, chosen at random from the mass function for a given morphological type, the bulge mass is assigned according to

$$M_0(\text{bulge}) = (\text{B/T}) M_0 + g\sigma_{\text{B/T}}, \tag{18}$$

TABLE 2

GIANT GALAXY PARAMETERS

	Luminosity Function			Bulge/Total Ratio	
Type	N_0	$\langle M \rangle$	σ_{LF}	Mean	$\sigma_{\text{B/T}}$
E	0.37	0.11	1.7	1.0	0.0
S0	1.15	0.11	1.7	0.4	0.25
Sab	2.00	0.35	1.1	0.3	0.27
Sbc.....	4.00	0.09	1.3	0.15	0.27
Sdm.....	8.00	0.0091	1.3	0.0	0.0

where g is a Gaussian random deviate with unit variance, as above. Our calibration of the fiducial mass ensures that the adopted B/T refers to the B_J band at redshift $z = 0$. The spectral dependence and evolution of B/T is automatically accounted for by the separate synthesis models for the bulge and disk components.

We adopt standard relations for the sizes of the locally observed galaxies. The Monte Carlo procedure allows us to introduce realistic scatter about the mean relations. For the bulges, we use the relation of Sandage & Perelmuter (1990). Because the total magnitude is evolving, we express the relation in terms of fiducial mass. Hence, the absolute magnitude that a galaxy *would* have, if it had an age of 1.3×10^{10} yr is

$$X = -2.5 \log M_0 - 21.1, \tag{19}$$

and the corresponding effective surface brightness is

$$Y = (-0.48X + 11.02)(1 + g). \tag{20}$$

As before, g is a Gaussian random deviate. The corresponding effective radius, for an $r^{1/4}$ law, is

$$r_e = 4.85 \times 10^{-8} \sqrt{10^{(Y - X - 0.75)/2.5}/\pi} \text{ kpc}. \tag{21}$$

For the disks, we use the Freeman value for the central surface brightness, with a 0.4 mag scatter,

$$X = -2.5 \log M_0 - 21.1, \tag{22}$$

$$Y = 21.6 + 0.4g. \tag{23}$$

The corresponding exponential scale length for the disk is

$$\alpha = 4.85 \times 10^{-8} \sqrt{10^{(Y - X)/2.5}/2\pi} \text{ kpc}. \tag{24}$$

All simulated galaxies associated with the locally observed population are assumed to form at $z = 5$, and their redshifts are assigned in a manner that ensures a constant comoving density.

3.3. *Distribution Functions for Dwarf Galaxies*

The properties of the dwarf population have already been discussed in § 2. The salient features are as follows:

1. The LF for the dwarfs is a power law, given by equation (7), with lower and upper mass cutoffs of 6×10^8 $M_\odot$ and 7.5×10^9 $M_\odot$, respectively. (The masses correspond to $V_c = 15$ and 35 km s^{-1} at $z = 1$.)
2. The dwarf galaxies begin to form at $z = 1$ and experience a short starburst of 10^7 yr. From equation (8), the fraction of dwarfs that have not experienced starburst in δt years after the beginning of the starburst epoch is

$$f(\text{dwarfs}) = e^{-\delta t/t_*}. \tag{25}$$

TABLE 3

DWARF GALAXY PARAMETERS

Model	M_{lower} ($10^8 M_\odot$)	t^* (10^8 yr)	ϵ	N_0 (Mpc^{-3})
1.....	6	20.0	0.03	4.0
2.....	6	50.0	0.03	4.0
3.....	6	1.0	0.03	4.0

3. According to equations (10) and (12), the flux from a dwarf galaxy of mass M at redshift z is

$$l(M) = l_0(M/M_0) , \quad (26)$$

where l_0 is the flux from a galaxy of mass $M_0 = 1 \times 10^9 M_\odot$ at the same redshift.

Within the framework outlined above, the essential free parameters are the star formation efficiency ϵ_* and the decay rate of the dwarf galaxy formation probability $1/t_*$. Less free, but still somewhat important, is the lower limit of the dwarf galaxy mass function, which is determined to within factors of a few by the ability of 10^4 K gas to collapse into low velocity-dispersion halos (Efstathiou 1992). Parameters for the different runs are shown in Table 3. N_0 in the table is the local space density of dwarfs integrated over the mass function.

We model the surface brightness distribution of the dwarf galaxies with an exponential profile whose scale length is derived from the collapse calculations described in § 2. Associating half-light radius with the half-mass (baryonic) radius and noting that the stellar systems in the dwarfs will expand during the epoch of mass loss, we set

$$r_e = 1.0(M/M_0)^{1/3} \text{ kpc for galaxy age } t < 1 \times 10^7 \text{ yr} , \quad (27)$$

and

$$r_e = 1.3(M/M_0)^{1/3} \text{ kpc for galaxy age } t > 1 \times 10^7 \text{ yr} . \quad (28)$$

We have modeled the expansion as a step function.

3.4. *Constructing Catalogs of Model Galaxies*

We construct a separate model-galaxy catalog for each of the galaxy types under consideration, selecting the galaxy parameters at random from the distribution functions described above. The procedure has been extensively tested to ensure that the input distributions are properly reproduced, even in the tails of the distributions. These catalogs list the redshifts, masses, and ages, the bulge r_e and disk α (in kiloparsecs and arcseconds), and magnitudes in various bands (for bulge and disk components, as well as the total) for each of the galaxies. The magnitudes are computed by integrating the properly redshifted and k-broadened spectra for the bulge and disk components through the filter bandpasses given in Bruzual (1981). The associated zero points are given in Ferguson & McGaugh (1995).

These separate catalogs are then processed by different programs that "observe" the galaxies using a given seeing and selection criteria. While observational results are usually quoted in terms of total magnitude, in practice galaxy detection is usually based on flux within a certain area above a certain threshold. To facilitate comparison with observations, we convolve the galaxies in our simulations with a Gaussian seeing profile with the FWHM quoted in the observational papers, then select galaxies and measure magnitudes in a way that closely matches the techniques in the surveys. The details of object selection and photometry in faint galaxy surveys are difficult to model precisely and sometimes are not completely specified in published reports. For those observational surveys that we have chosen to compare to, we list the associated selection criteria in Table 4 (see Ferguson & McGaugh 1995 for more details).

The galaxies that pass the selection criteria are then used to compute the LF, the number-magnitude counts $N(M)$, the redshift distribution $N(Z)$, etc. Galaxies of different morphological types are combined by weighting the contribution of each galaxy by $N_0(\text{type})/N_{\text{catalog}}(\text{type})$, where $N_{\text{catalog}}(\text{type})$ is the density of galaxies in the input catalog. For normal galaxies, $N_{\text{catalog}}(\text{type})$ is computed using all the galaxies in the volume out to $z = 5$. For the dwarfs, $N_{\text{catalog}}(\text{type})$ is computed from the number of galaxies with $z < 0.1$, to allow for the fact that the space density is evolving.

Our simulations do not explicitly include noise that is present in real observations. To the extent that the algorithms used to detect galaxies in deep surveys are unbiased, the effect of noise is simply to increase the scatter in the measured magnitudes. For the purpose at hand, a scatter of a few tenths of a

TABLE 4

ASSUMED SURVEY PARAMETERS

Observer	Band	Magnitude	Seeing	D_{min}	μ_{lim}	Remarks
Loveday et al. 1992	B_J	Isophotal	3.″0	...	24.5	1
Tyson 1988	B_J	Isophotal	1.2	...	28.7	
Colless et al. 1993	B_J	Isophotal	1.0	...	26.5	2
Lilly 1993 $N(m)$	I_{AB}	Hybrid	1.2	2.″0	28.0	3
Lilly et al. 1995 $N(z)$	I_{AB}	Aperture	0.7	3.0	28.0	4
Cowie et al. 1994 K-band $N(m)$	K_{AB}	Aperture	1.0	3.0	25.4	5
Djorgovski et al. 1995 K-band $N(m)$.....	K_{AB}	Aperture	0.75	1.5	25.8	6
Songaila et al. 1994 K-band $N(z)$	K_{AB}	Aperture	0.6	3.5	28.63	7
Glazebrook et al. 1995	B_{AB}	Isophotal	2.26	1.6	26.6	8

NOTES.—(1) Correction of -0.27 added to isophotal magnitudes. (2) Correction of -0.58 added to isophotal magnitudes. (3) Isophotal magnitudes for galaxies with $D_{28} > 2''$; otherwise, used $2''$ aperture. (4) Assumed complete to $D_{28} > 2''$; $3''$ aperture used. (5) Assumed complete to $D_{25.4} > 1''$. Isophotal magnitudes used. (6) Selection is roughly by total magnitude, as the details are not specified. Magnitudes are within a 1.″5 diameter aperture, with a constant of -0.275 added. (7) We use magnitude limits $19.8 < K_{AB} < 20.8$ (Songaila et al. 1994 use K rather than K_{AB}), and measure magnitudes in an aperture of 1.″75 radius. We have not attempted to match the Songaila et al. 1994 isophotal selection criteria, as they varied from field to field (see Cowie et al. 1994). (8) While galaxies are selected by isophotal diameter, magnitudes are computed in a 4.″0 diameter aperture with a constant -0.3 mag correction to total magnitude (this varied slightly from night to night in the real survey).

magnitude is unimportant. In any case, the best way to assess the impact of noise would be to construct simulated images with noise and analyze them in the same way as the observations. Such an analysis will be presented in a separate paper, in which we perform a detailed comparison of the model predictions with results from deep, high-resolution observations from *HST* and the New Technology Telescope (ESO, Chile) (NTT) (Ferguson et al. 1995).

4. RESULTS

4.1. *Evolution of a Starburst Dwarf Galaxy*

Figure 5 shows the evolution of the spectral energy distribution for a $10^9\ M_\odot$ dwarf that experiences a 10^7 yr starburst, during which time it forms stars of metallicity $Z = Z_\odot/20$ at the rate of $3\ M_\odot\ \mathrm{yr}^{-1}$. During the starburst, the galaxy spectrum is quite steep ($f_\nu \propto \nu$), with the UV light being largely due to short-lived massive stars. Once the starburst ceases and the number of massive stars declines, so does the UV luminosity. The spectral energy distribution becomes increasingly dominated by longer-lived but nonetheless aging, less massive stars. Figure 6 illustrates this more clearly. The top panel shows the evolution of the rest-frame M_{B_J} (*solid curve*) and $M_{K_{AB}}$ (*dashed curve*) as a function of time. After the cessation of star formation, the *B*-band luminosity of the galaxy fades by as much as 6 mag over a span of 10^{10} yr. At longer wavelengths the fading is more tempered. The lower panel of Figure 6 shows the time evolution of the dwarf galaxy's rest-frame $B_J - K_{AB}$ and $B_J - I_{AB}$ colors. Based on these color curves, we can anticipate the conclusion of the next section, that the bursting dwarfs, which dominate the counts at $B > 25$, will not contribute significantly to the *I*- and *K*-band counts until near the limits of current surveys.

4.2. *Evolution of Normal Galaxies*

Figure 7 shows the evolution of the rest-frame B_J and K_{AB} magnitudes for E, S0, Sab, Sbc, and Sdm galaxies with present-

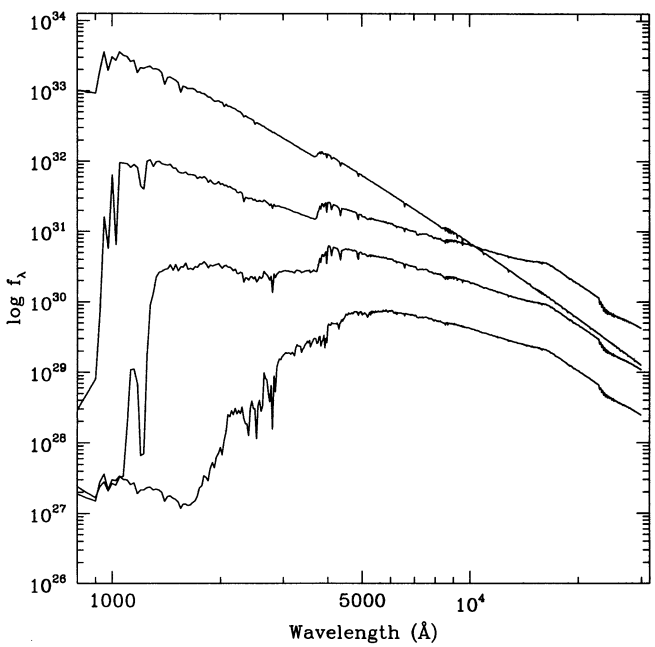

FIG. 5.—Evolution of the spectral energy distribution of a $10^9\ M_\odot$ dwarf galaxy that experiences starburst at the rate of $3\ M_\odot\ \mathrm{yr}^{-1}$ for 10^7 yr. Different curves correspond to the spectral energy distributions at ages 10^7, 10^8, 10^9, and 10^{10} yr. We assume that the metallicity of the stellar population is $Z = 0.001$.

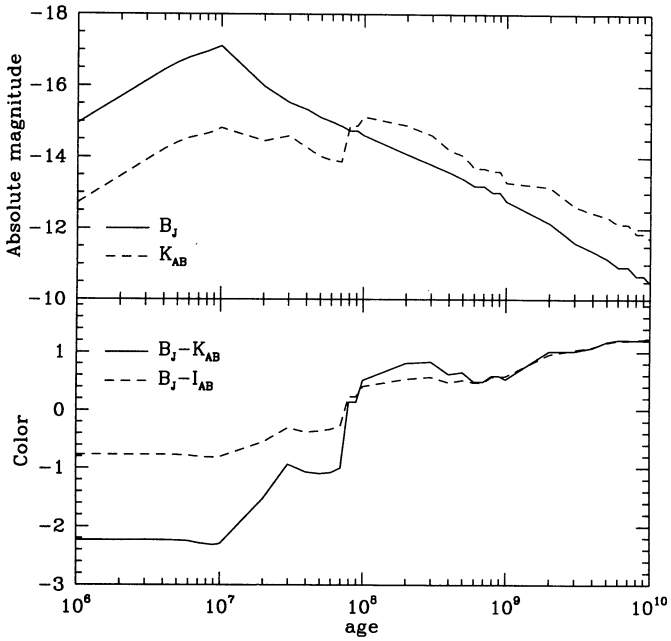

FIG. 6.—*Upper panel*: Time evolution of the rest-frame M_{B_J} (*solid curve*) and $M_{K_{AB}}$ (*dashed curve*) for a starburst dwarf galaxy. In the optical, the galaxy fades by as much as 6 mag after the quenching of the starburst. In the infrared, the galaxy fades by as much as 4 mag below the maximum. *Lower panel*: Time evolution of the rest-frame $B_J - K_{AB}$ and $B_J - I_{AB}$ colors for the dwarfs. Well after the burst phase, the $B_J - K_{AB}$ and $B_J - I_{AB}$ colors are comparable. Based on these color curves, the faint bursting dwarfs are not expected to contribute significantly to the *I*- and *K*-band counts until near the limits of current surveys.

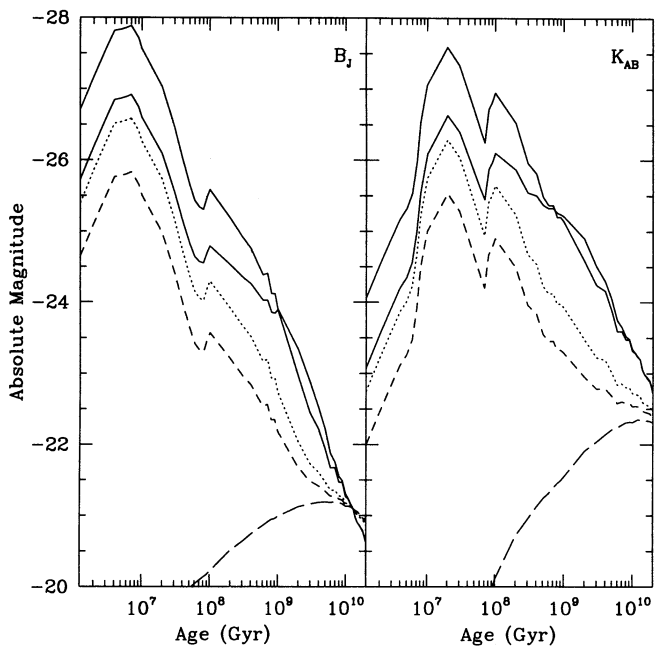

FIG. 7.—Evolution in B_J and K_{AB} band luminosity for different types of normal galaxies. The solid curves show E and S0 galaxies, dotted curves Sab, short-dashed curves Scd, and long-dashed curves Sdm galaxies. The spiral galaxy luminosities are all shown for the mean bulge/disk ratio. In our models, the spaces between the curves are filled as well, because of the distribution in bulge/disk ratio.

day luminosity $M_{B_J} = -21$ and bulge/disk ratios at the means for each type. Because spiral galaxies in our models consist of bulge and disk components drawn from rather broad distributions in relative luminosity, in practice the normal galaxies in our models fill in the whole range of colors from E to Sdm galaxies. At early times $t < 1$ Gyr, the photometric evolution is dominated by the bulge component, while at late times colors are primarily governed by the bulge/disk ratio. Obviously, the evolution in luminosity shown in Figure 7 includes no merging. However, as long as *most* of the merging that formed ellipticals and bulges occurred above redshifts $z \approx 2$ (Kauffmann 1995), the photometric evolution will be essentially identical by $z = 1$ (the limits of current redshift surveys). At $z \approx 1$, the distribution of $\mathscr{R} - K$ colors in our models is consistent with that observed in samples of galaxies selected by virtue of Mg II absorption in the spectra of QSOs (Steidel et al. 1994; Steidel & Dickinson 1994). At lower redshifts, the luminosity evolution of all galaxy types in our model is modest. With respect to the present-day luminosity, the galaxies at $z = 1$ are 0.1–0.7 mag brighter in rest-frame B_J. In the K band, the evolution ranges from -0.3 to 0.6 mag.

4.3. *The Number-Magnitude Counts*

Having described the evolution of individual galaxy types, we now turn to the collective properties of the complete galaxy sample. We begin by comparing the number-magnitude trends predicted by the model with observations. In Figure 8, we plot the data for the number counts in B_J ($\approx B_{AB} - 0.07$), I_{AB}, and K_{AB} bands drawn from various sources, as well as the number-magnitude relationship for a nonevolving population of locally observed galaxies (hereafter referred to as the NE model). Comparing the observed B-band counts versus the NE model, one finds that by $B_{AB} = 24$ the NE curve falls short by a factor of 4. The $N(M)$ relations for our models, computed using total magnitude selection, are shown for different values of t_*, the formation timescale for the dwarf population. Bearing in mind that curves are computed on the basis of total magnitudes and that the incorporation of selection effects only acts to decrease the number of galaxies observed at a given magnitude, it is evident that formation timescales as short as 10^8 yr (i.e., most of the dwarf galaxies form very soon after $z \approx 1$) are not favored. This conclusion will be further strengthened when we consider the corresponding redshift distribution. It is, however, important to point out that all the models predict that the K counts ought to begin rising somewhat more steeply at magnitudes fainter than $K_{AB} \approx 24$–25. This is a generic feature of the bursting dwarf model.

Choosing model 1 ($t_* = 2 \times 10^9$ yr) as our fiducial model, we compute the $N(m)$ in the different bands according to the selection criteria summarized in Table 4. The results are shown in Figure 9. The model number counts (*solid curve*) are in very good agreement with observations in all three bands. For comparison, we also plot the number counts computed with total magnitude selection, as well as the NE model curve. The effect of selection on these models is to flatten the observed $N(m)$ relation at faint magnitudes near the limits of ground-based surveys. In Figure 10, we decompose the number counts associated with model 1 (total magnitude selection) into counts due to the evolving, locally observed galaxy population (*dotted curve*) and the starbursting dwarf population (*dashed curve*). In the B band, the excess (with respect to the NE model) of galaxies in the range $18 \lesssim B_{AB} \lesssim 23$ is largely due to the evolving population of locally observed galaxies. Thereafter, the starbursting dwarfs become increasingly important. Thirty percent

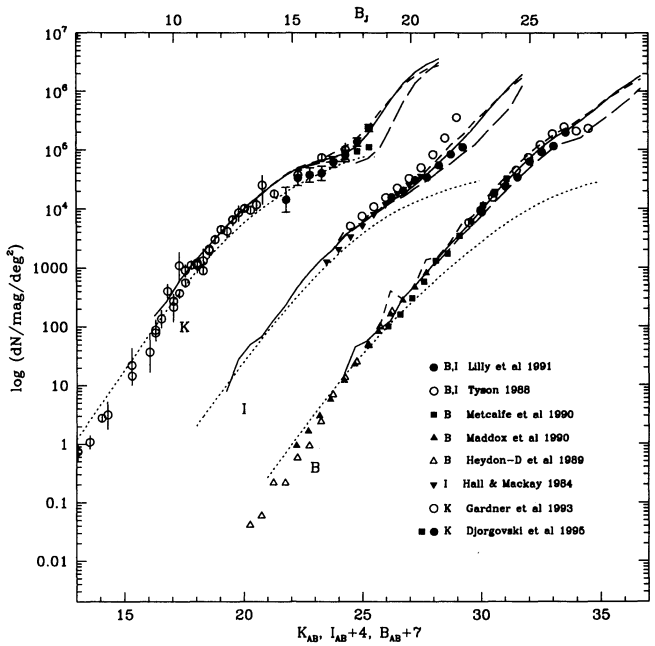

FIG. 8.—Galaxy number counts for the bursting dwarf models compared to the data (*points*) and the standard no-evolution model (*lower dotted curve*). Bursting dwarf models are shown for three different values of t_*, the e-folding time of the probability of collapse of the baryonic component of a dwarf galaxy halo. The curves are solid, short-dashed, and long-dashed for $t_* = 2 \times 10^9$, 5×10^9, and 1×10^8 yr, respectively.

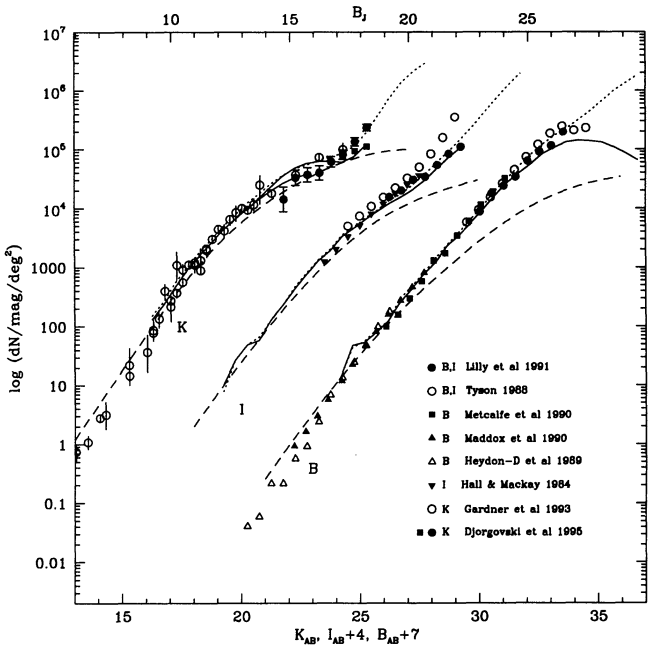

FIG. 9.—Galaxy number counts for the bursting dwarf with $t^* = 2 \times 10^9$ yr, compared to the data (*points*), now with the appropriate survey selection criteria and magnitude estimation techniques applied (*solid curves*). Also shown are the standard no-evolution model (*dashed curves*) and the dwarf model selected by total magnitude (*dotted curve*). In the K band, two solid curves are shown, one for Cowie et al. (1994), and one for the very deep counts from Djorgovski et al. (1995).

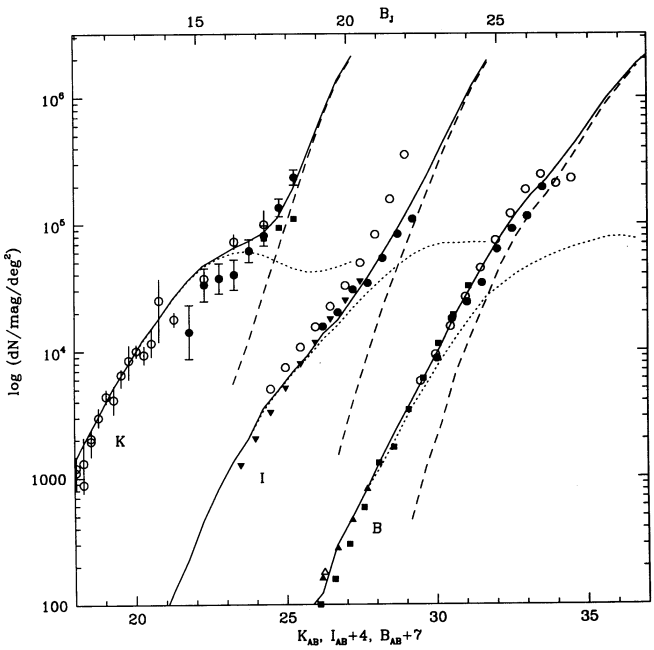

FIG. 10.—Number counts decomposed into giants (*dotted curves*), dwarf (*dashed curves*), and total (*solid curves*). All selected according to total magnitudes.

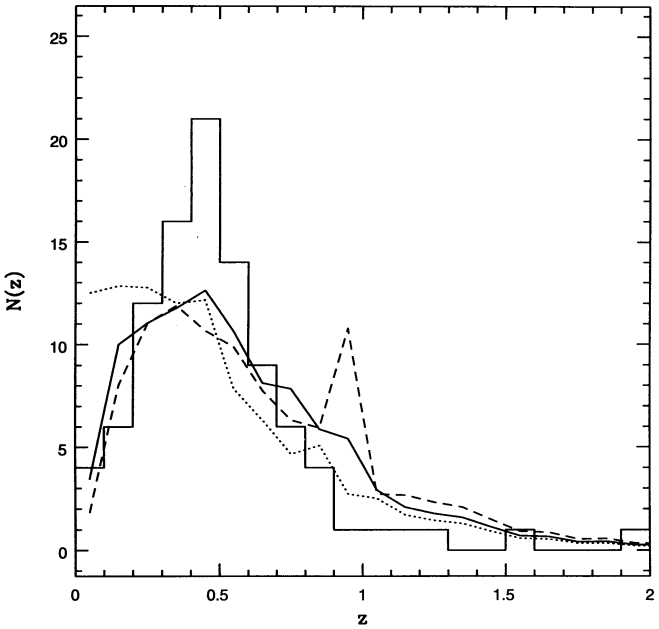

FIG. 11.—$N(z)$ relation for the three models. The histogram shows the data from Glazebrook et al. (1995). *Solid curve*: model 1 ($t_* = 2 \times 10^9$ yr); *dotted curve*: model 2 ($t_* = 5 \times 10^9$ yr); *dashed curve*: model 3 ($t_* = 10^8$ yr). All curves are normalized between redshifts of 0 and 2.

of the galaxies $B_{AB} \leq 24$ are starbursting dwarfs, and the fraction increases toward fainter magnitudes. The same is true for the excess in the I band ($18 \lesssim I_{AB} \lesssim 23$). The fraction of dwarfs in an $I_{AB} \leq 23$ sample is approximately 15%. It should be noted that the dwarf fraction does not take into account the contribution of other small but normal evolving galaxies such as the Sdm's.

4.4. *The Redshift Distribution*

From the above discussion it is clear that the dwarf galaxies in these models do not dominate the counts at the limits probed by current redshift surveys. *The bursting dwarf galaxy model cannot by itself resolve the discrepancy between the $N(z)$ and $N(m)$ relations in the range* $20 < B < 24$. Thus, comparison to the redshift distributions only weakly test the dwarf galaxy aspect of the model. Such comparisons mostly test our treatment of selection biases and the modifications we have made to the standard passive-evolution model (the inclusion of separate bulge and disk components with a distribution function in fractional contribution to the total light, and the incorporation of dust at early epochs).

In Figure 11 we compare the predicted redshift distribution to the observations for three values of t_*, where the galaxies were subject to the selection criteria of the Glazebrook et al. (1995) survey. The model distributions are normalized so that the number of galaxies in the redshift range $0 \leq z \leq 2$ matches that in the survey. This comparison provides our primary constraint on t_*. Models with a prolonged epoch of dwarf galaxy formation ($t_* \approx 5 \times 10^9$ yr) overpredict the number of low-redshift galaxies that would be detected at $B = 24$, even with the appropriate selection effects taken into account. On the other hand, models with a very short epoch of formation ($t_* \approx 10^8$ yr) predict a pronounced peak in the redshift distribution at the redshift of formation of the dwarfs. The model with a moderate formation timescale, $t_* = 2 \times 10^9$ yr, yields a redshift distribution that is in reasonable agreement with the observations.

While the peak of the redshift distributions in the models and the data agree very well, in all cases, the model distributions appear somewhat flatter than the observed distribution. As the Glazebrook et al. (1995) redshift survey is only 73% complete, inconsistency at the level shown in Figure 11 is not a problem and, indeed, is *expected* if the unidentified galaxies tend to lie at higher redshifts. Glazebrook et al. (1995) discuss the possible redshift distribution of the unidentified sources (sources brighter than the $B = 24$ mag limit that were detected but whose redshifts were not obtained). They conclude that the unidentified sources are most likely to be a mixture of weak-lined sources in the redshift range $0 < z < 1$ and galaxies with $z > 1$, for which [O II] is shifted out of the spectral window. The color distribution of the unidentified objects favors the interpretation that they are mostly late-type galaxies at $z > 0.5$.

In Figure 12 we present the redshift distributions associated with our fiducial model (model 1: $t_* = 2 \times 10^9$ yr), computed using different selection criteria. Selection criteria and magnitude estimation schemes resemble those used in the real surveys (Colless et al. 1993; Lilly 1993; Glazebrook et al. 1995; Songaila et al. 1994), and the models are normalized to the data over the redshift range shown. The most complete surveys, those by Colless et al. (1993) and Lilly et al. (1995) show good agreement with the models, while the deeper, less complete surveys show distributions more sharply peaked at $z \sim 0.5$ than the models, which may be an artifact stemming from the difficulty of obtaining redshifts for galaxies at higher redshift.

We conclude by emphasizing that the redshift distributions primarily test our adopted models for the evolution of normal galaxies. Table 5 shows the relative contributions of different galaxy types to the redshift distributions shown in Figure 12.

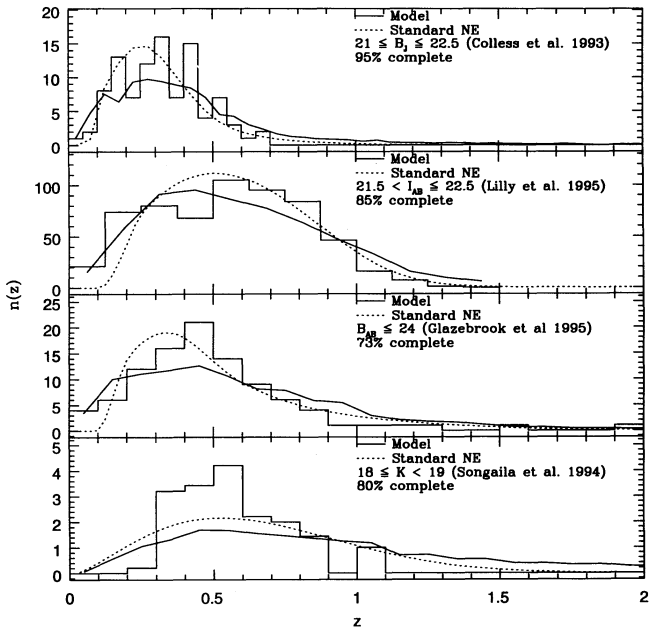

FIG. 12.—$N(z)$ redshift distribution for our fiducial ($t^* = 2$ Gyr) model, compared to the data from various surveys. Models have been normalized to match the total number of objects observed in the redshift range $0 < z < 2$. The number of galaxies predicted with $z > 2$ ranges from 4% to 12%, being highest for the Lilly et al. (1995) selection criteria. The K-band redshift sample consists of galaxies observed in fields SSA4, SSA13, SSA17, and SSA22 by Songaila et al. (1994), with the number of galaxies normalized to account for variations in area coverage over the magnitude range $18 < K < 19$ (hence there are nonintegral numbers of galaxies in the plot).

Bursting dwarf galaxies in the model contribute significantly only to the Glazebrook et al. (1995) survey. Given the incompleteness, the only distribution that appears problematical is the K-band sample of Songaila et al. (1994). However, that sample contains only 24 galaxies, so a definitive test will have to await the results of larger surveys.

Why have previous passive-evolution models for normal galaxies predicted a high-redshift tail? The attempt to match the counts at very faint magnitues ($B > 25$) forces such models to have the galaxies visible during the star formation phase (i.e., not hidden by dust) and to have a rather prolonged epoch of formation [so as not to produce a feature in the $N(m)$ distribution]. While such a galaxy formation scenario is plausible (see, for example, Guiderdoni & Rocca-Volmerange 1990), it is by no means a unique way to arrive at the colors of present-day normal galaxies. By providing an alternative explanation for the very faint galaxies, our model removes the requirement that normal galaxies, particularly the giant galaxies, be visible during their formation phase. For a redshift of formation $z_f \approx 5$, it is galaxies with star formation timescales $\tau \approx 1 \times 10^9$ yr that are most problematical for the redshift distributions. Such galaxies do not fade sufficiently by redshifts of 1–3 to disappear from the redshift distribution. By including dust during the star formation epoch of ellipticals, bulges, and S0 disks, we have quite consciously *tuned* the models to remove the high-redshift tail. The required optical depths are modest (peaking at $\tau = 1$ in the rest-frame B band). While other explanations for the lack of high-redshift galaxies in the existing deep surveys are clearly possible, we contend that existing redshift surveys do not require serious modifications to passive-evolution models or to the idea that the normal galaxy population formed largely at redshifts significantly greater than unity.

TABLE 5

PERCENT CONTRIBUTION OF DIFFERENT MORPHOLOGICAL TYPES TO $N(z)$

Survey	Band	E + S0	Sab + Sbc	Sdm	Dwarf
Colless et al. 1993	B_J	14	67	7	12
Lilly et al. 1995	I	29	65	5	1
Glazebrook et al. 1995.....	B	14	53	6	27
Songaila et al. 1994	K	41	57	2	0

For illustrative purposes, we plot the redshift distribution of galaxies brighter than $B_J = 26$ for our fiducial model in Figure 13. We simply selected the galaxies on the basis of total magnitudes, since there are no redshift surveys that reach such faint magnitudes. Three features of the redshift distribution are noteworthy. First, the low-redshift peak is due to relatively nearby, fading dwarf remnants. As long as the galaxies are selected on the basis of total magnitudes, this peak is present even if the threshold magnitude is raised to $B_J = 24$. Real surveys, however, tend to be biased against LSB objects and therefore cannot detect these remnants. (Note the lack of a low-redshift peak Fig. 12.) Second, the tail at $z > 1$ is entirely due to a passively evolving, locally observed population of galaxies. Third, the peak at $z \approx 1$ is due to a starbursting dwarf population. This peak sharply cuts off at $z = 1$ because of our fiat that dwarf halos form stars only at $z \leq 1$.

4.5. *Luminosity Function*

In Figure 14 we plot the overall present-day LF for galaxies in model 1, selected by total magnitude as well as by the isophotal selection criteria of the Loveday et al. (1992) survey. We also plot the LFs for each morphological type. As noted previously (§ 3.2), the LFs for the different galaxy types, with the exception of the dwarfs, are Gaussian, with parameters chosen such that the individual LFs approximate those shown in Binggeli et al. (1988), while the overall LF has a Schechter

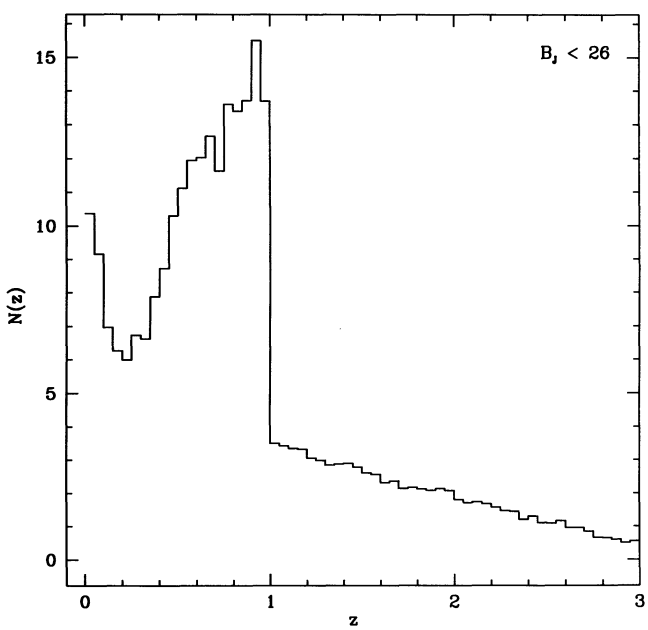

FIG. 13.—$N(z)$ relation for a hypothetical survey selected by total magnitude to $B_J = 26$.

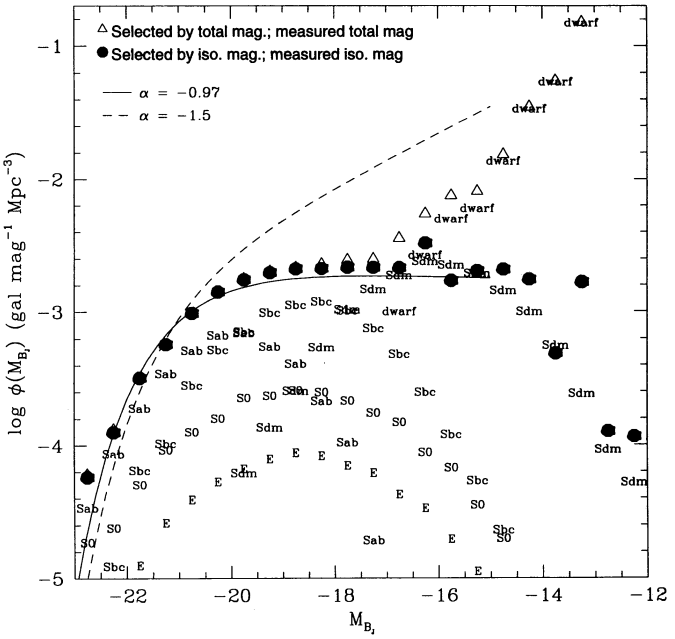

FIG. 14.—Local LF of galaxies of different types predicted by model 1. Solid symbols show the total LF predicted for a survey with the selection criteria of the Loveday et al. (1992) survey. Open triangles show the LF that would be derived in a survey with *no isophotal threshold* (i.e., an ideal survey with no sky background or detector noise). The LF, for the individual morphological types are labeled by their Hubble class. The solid line shows a Schechter function with $\phi^* = 2.3 \times 10^{-3}$ Mpc^{-3} and $\alpha = -0.97$. The dashed curve is a Schechter function with $\alpha = -1.5$ and the same ϕ^*. The total LF derived by Loveday et al. (1992) had a slope $\alpha = -0.97$ but a lower normalization.

(1976) function profile over the range $M_{B_J} = -23$ to -16.5, the limit of the Loveday et al. (1992) survey for $H_0 = 50$ km s^{-1} Mpc. Over this magnitude range, the isophotal selection yields similar results to total magnitude selection.

The presence of dwarfs in model 1 causes the total magnitude LF to steepen at magnitudes fainter than $M_{B_J} = -16$. There is some evidence for such a rise in the local galaxy LF. Ferguson & Sandage (1991) found that the LF in nearby loose groups turns up below $M_B = -16$, with the faint end being dominated by LSB dE galaxies. More recently, the LF of galaxies in the $m_Z \leq 15.5$ CfA Redshift Survey (Marzke, Huchra, & Geller 1994) also shows an indication of such a rise, as does the LF in rich clusters of galaxies (De Propris et al. 1995). The ability to detect the predicted turnup in the LF depends sensitively on the selection criteria of the survey. For example, the LF recovered from our simulated catalogs using the isophotal selection criteria of the Loveday et al. (1992) survey shows no evidence of the steepening, in spite of the large number of low-luminosity dwarfs present in model 1.

While their space density is high, the luminosity density for the faded dwarfs is significantly lower than for the normal galaxies. Adding up the light from the galaxies in the simulated catalogs used to produce Figure 14, we arrive at estimates in the B_J band of 1.1×10^8 $L_\odot$ Mpc^{-3} for the normal galaxies and 3.3×10^7 $L_\odot$ Mpc^{-3} for the dwarfs. In the K band, the numbers are 4.9×10^8 and 1.7×10^7, respectively. Thus the dwarfs constitute from 3% to 30% of the luminosity density of the local universe, depending on the bandpass.

Looking back toward $z \approx 1$, the "regular" galaxies experience very modest luminosity evolution, with galaxies being brighter by 0.1–0.7 mag in rest-frame B_J and -0.3–0.6 mag brighter in the K band.

4.6. *Color Distributions*

The comparison of the observed versus model color distributions provides an additional test of the model. In Figure 15 we compare the model 1 galaxy colors to those observed by Lilly, Cowie, & Gardner (1991). Applying their selection criteria, the galaxies were required to have $20 < I_{AB} < 25$ and $B_{AB} < 27$ through a 3″ aperture in a 1.″2 seeing. The mean $B_{AB} - I_{AB}$ color is 1.51 in the data and 1.26 in the models, with most of the difference lying in the tails of the distribution. The peak of the color distribution agrees to within 0.2 mag. The model galaxy sample consists of 27% dwarfs. Hence, the color distribution at these magnitude limits primarily tests the assumptions we have made for the evolution of normal galaxies. At fainter magnitudes, the colors become rapidly bluer as the dwarf galaxies begin to dominate the numbers. This trend is very much in keeping with that illustrated in Figure 2 of Koo & Kron (1992), which shows that the color distribution of galaxies with $B_J \lesssim 23$ is similar to that of the nearby galaxies, while at fainter magnitudes, the distribution shifts significantly toward the blue.

In Figure 16 we plot $I-K$ (Johnson system) color versus K magnitude for model 1 galaxies selected at random from the simulated catalogs, with $I_{AB} < 25.48$ and with a sample size equal to that of Djorgovski et al. (1995). This is the equivalent of their Figure 4 and is broadly consistent, although perhaps lacking somewhat in blue galaxies, with $K < 21$. We particularly draw attention to the fact that the models do not predict an overabundance of very blue galaxies at the faint limits, in spite of the fact that the dwarfs are predominantly very blue.

4.7. *Effective Radii*

For $q_0 = 0.5$, the angular size versus redshift relation has a minimum at $z \approx 1.2$. The counts at the limits of ground-based surveys in our models are dominated by dwarf galaxies with

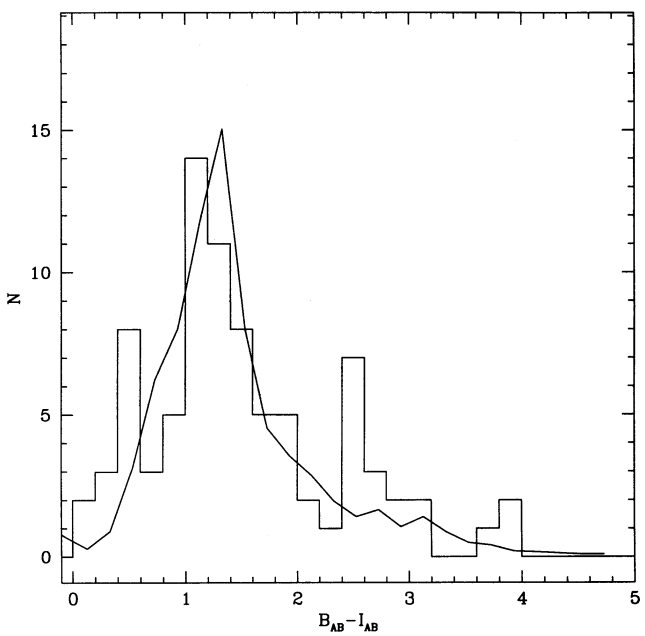

FIG. 15.—Comparison of the predicted $(B-I)_{AB}$ color distribution from model 1 with observations of Lilly et al. (1991).

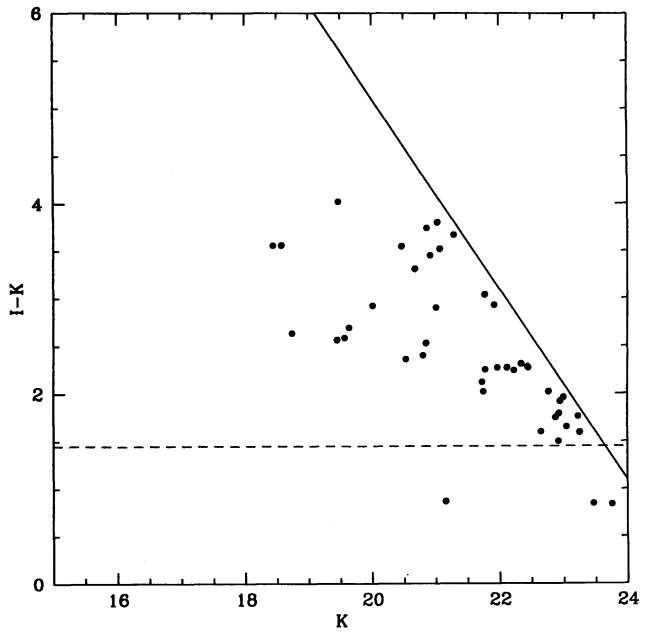

FIG. 16.—Predicted Johnson $I-K$ color for galaxies brighter than $I_{AB} = 25.48$.

effective radii ~ 1 kpc at redshifts $0.5 \lesssim z \lesssim 1$. At these redshifts, the angular effective radii of the dwarf galaxy population are a few tenths of an arcsecond. The angular size distribution predicted by our models probably comes close to the extreme that could be expected for *any* model with a geometrically flat universe. While we reserve detailed size comparisons to a later paper (Ferguson et al. 1995), in Figure 17 we show comparison to recent measurements from the MDS (Griffiths et al. 1995) in the magnitude range $21 < I < 22$. If anything, the models contain *too few* galaxies with effective radii less than 0".5. We have not attempted to duplicate the MDS selection criteria, and it is possible the selection criteria may tend to favor the detection of galaxies with small effective radii due to their higher surface brightnesses. In any case, at $I = 22$, the models are still dominated by normal galaxies. The predicted distribution at fainter magnitudes is shown in Figure 18.

5. DISCUSSION

The tests in the previous section show that the "boojums as starbursting dwarfs" model satisfies the available constraints from ground-based measurements of the number counts, redshift distributions, and colors of faint galaxies, and shows qualitative consistency with early *HST* measurements of angular sizes. Admittedly, the success is partly due to parameters that are not well constrained. For the normal galaxies, the ad hoc inclusion of dust during the star formation epoch cures the tendency for passive-evolution models to overpredict the number of high-z galaxies in deep redshift surveys. For the dwarfs, the parameter t_* hides our ignorance of the detailed evolution of the ionizing background and the distribution of gas density profiles in proto–dwarf galaxy halos. To match the counts and redshift distributions, t_* must be approximately $(2 \pm 1) \times 10^9$ yr. Having, to a certain extent, adjusted the models to fit the data, the agreement of the model color and size distributions with the data provides some confirmation that our assumptions are correct. However, the tests performed in this paper do not prove that bursting dwarf galaxies are the correct solution to the faint blue galaxy problem, merely that the hypothesis is not ruled out.

5.1. *Pros and Cons of the Model*

From a theoretical perspective, there are several attractive features to the bursting dwarf model. First, the mass function and space density of dwarf galaxy halos are *not* free parameters, having been fixed by the adoption of a realistic power spectrum such as the CDM power spectrum to describe the

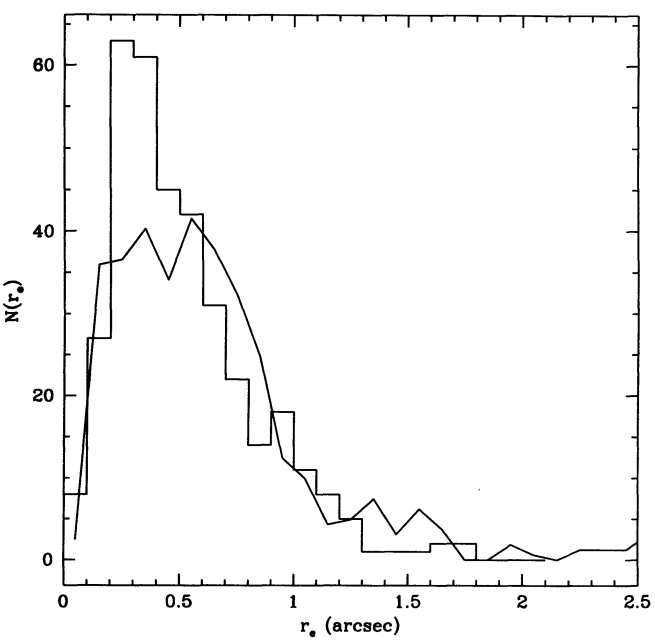

FIG. 17.—Effective radius distribution for model 1 (*curve*) compared to the observed distribution from the MDS (Griffiths et al. 1995) in the magnitude range $21 < I < 22$.

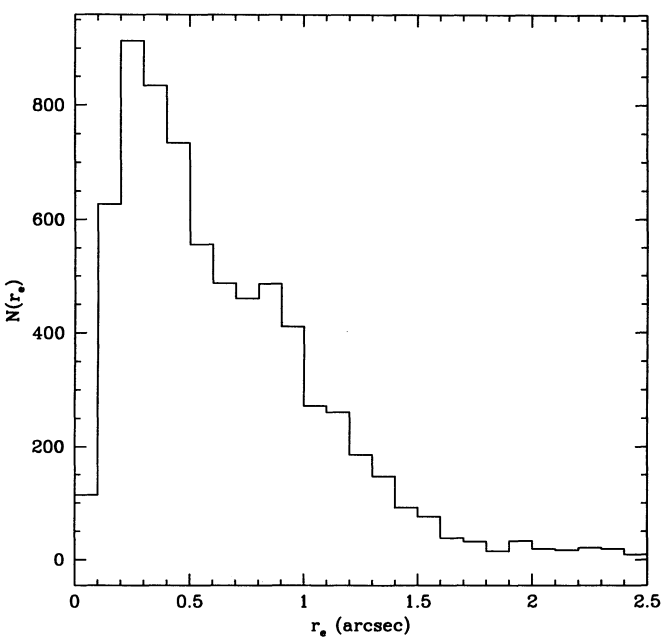

FIG. 18.—Predicted effective radius distribution from model 1 for galaxies brighter than $I_{AB} = 25$.

initial density fluctuations on galactic and subgalactic scales. Second, the model links in a natural way the low-density gas probed by QSO absorption lines at high redshift and the faint blue galaxy population seen at moderate redshifts. Third, dwarf galaxies are expected to be less clustered than larger ones (Efstathiou 1995), which at least goes in the right direction toward explaining the low amplitude of the angular correlation function at faint magnitudes. Fourth, a specific triggering mechanism (the drop in the ionizing UV background at $z \approx 1$) has been identified that would promote cooling and star formation in low-mass gas clouds at moderate redshift. Tidal interactions are assumed to provide the triggering in other dwarf-dominated models (Lacey et al. 1993; Kauffmann et al. 1994), but the details are left unspecified. Fifth, the angular size distribution of the dwarf galaxies is expected to be peaked at small scale, in qualitative agreement with recent results from the *HST* MDS (Im et al. 1995). Finally, because wholesale merging is not required in the models, normal galaxies, particularly the giant galaxies, can follow standard passive-evolution tracks in color and luminosity versus redshift, as favored by observations of cluster ellipticals (Aragón-Salamanca et al. 1993; Rakos & Schombert 1995; Dickinson 1995) and luminous field galaxies (Colless 1994; Steidel & Dickinson 1995).

While the model does not contradict any specific observations, there are circumstantial arguments *against* the "boojums as starbursting dwarfs" hypothesis:

1. We must postulate that the faded remnants of the bursting dwarf population, while populating the local universe at a density of $\sim$2–4 Mpc^{-3}, are for the most part unobserved. Their structural properties are similar to those of the local group dwarf spheroidals, but their star formation histories are different. The Local Group dSph galaxies all show evidence for an old (globular cluster age) population, by virtue of RR Lyrae stars, and, hence, argue against the hypothesis that the formation of low-mass galaxies is suppressed by the background UV flux.

On the other hand, hierarchical clustering models also predict that low-mass density peaks that reside in regions destined to form groups and clusters will virialize at earlier epochs than those residing in the "field." As we noted in § 2, typical (i.e., 1 σ) peaks on a $10^9\ M_\odot$ scale in an $\Omega = 1, \sigma_8 = 0.67$ CDM universe, for example, virialize at $z \approx 3.5$, whereas 2 σ peaks of the same mass scale virialize at $z \approx 8$. If the universe is not photoionized at the time when the high peaks form virialized structures, then the resulting halos will certainly experience starbursts soon after virialization. In addition, halos that form at higher redshifts are more compact. At $z = 8$, for instance, a virialized $10^9\ M_\odot$ halo has a circular velocity of $V_c = 38$ km s^{-1}; even if the universe is photoionized at this epoch, the $T \approx 3 \times 10^4$ K gas will not remain "stably confined" in such halos but will cool and eventually form stars. It is quite likely that the Local Group dwarf spheroidals do not correspond to "typical" peaks but, rather, high-σ peaks. It should be noted that high peaks are expected to be strongly clustered. Furthermore, it should also be noted that the peculiar episodic star formation histories of the Local Group dSphs are problematic for any model of galaxy formation.

2. Recent evidence for metal enrichment in the Lyα forest (Tytler 1995; Cowie et al. 1995) suggests that the intergalactic gas is not of primordial abundance. It is not clear, therefore, whether the metagalactic radiation field will be able to overcome the more efficient cooling. However, the detections indicate that the metal abundance in the Lyα forest is $\sim 0.01\ Z_\odot$, and, for such low values of Z, the cooling function of the gas is not significantly different from that for gas of primordial abundance, since the cooling is dominated by hydrogen and helium recombination line radiation.

3. In our models, the faded remnants of the boojum population are LSB galaxies that have ejected all their gas. In contrast, nearby LSB galaxies outside of clusters are generally gas rich. For example, 77% of the optically selected LSB galaxies studied by Eder et al. (1989) were detected in H I at 21 cm. On the other hand, the Eder survey is almost 100% incomplete for diameters less than 40″, the very regime where the faded boojums are expected to be found.

5.2. *Tests of the Bursting Dwarf Hypothesis*

Fortunately, the model does not stand or fall on the above arguments. There are a number of observations that can provide a test of the bursting dwarf scenario, without being particularly sensitive to our specific assumptions about star formation histories, dust, metallicities, or effective radii. We outline some of these tests below.

1. *The redshift distribution at very faint magnitudes should show a peak near $z = 1$.*—With most of the star formation activity occurring between redshifts $0.5 \lesssim z \lesssim 1$, the bursting dwarf model makes a unique prediction for the redshift distribution at magnitudes $B > 25$, where the dwarf galaxies dominate the counts. The exact shape of the peak in the redshift distribution shown in Figure 13 is determined by t_* and our assumption that the dwarfs do not form before $z = 1$. However, even a more realistic spread in formation redshifts to $z > 1$ will not remove the pronounced peak.

2. *The K-band counts should continue to rise to $K_{AB} = 28$.*—Passive-evolution models with $q_0 = 0.5$ are able to match the K-band counts down to magnitudes $K_{AB} \approx 24$, but predict continued flattening of the $N(m)$ distribution to fainter magnitudes. In contrast, the bursting dwarf model predicts that the slope of the $N(m)$ distribution should stay constant or even rise fainter than $K = 24$. The near-infrared light from the bursting dwarfs counteracts the expected decline in slope. It is worth noting that the dwarfs fade in the K band, as well as the optical bands, and provide most of their contribution to the counts near the starburst epoch. Thus, the predicted redshift distribution at $K_{AB} \approx 25$ is similar to that at $B_{AB} = 25$.

3. *The angular diameters of galaxies should continue to decrease with magnitude.*—In our models, the effective radii of the dwarfs are $\sim$1 kpc and vary by a factor of $\sim$10 over the LF. At $z = 1$, a galaxy with $r_e = 1$ kpc would have an observed $r_e = 0\farcs1$, near the limits of *HST* resolution with the WF/PC. Because the counts in the bursting dwarf scenario are dominated by galaxies near the minimum of the $\theta(z)$ relation, the predicted angular sizes are probably the smallest that could be anticipated in *any* plausible model of galaxy evolution with $q_0 = 0.5$.

4. *The local field LF from surveys with total magnitude selection ought to exhibit a steeply rising turnup at magnitudes fainter than $M_B \approx -16$.*—The exact magnitude at which this rise begins will depend on the details of the star formation histories, and whether or not this upturn is detected depends sensitively on the selection criteria of the survey. For example, the LF recovered from our simulated catalogs using the isophotal selection of the Loveday et al. (1992) survey shows no evidence of the steepening, in spite of the large number of low-luminosity dwarfs being present.

5. *Faded, LSB remnants of the boojums population should be detectable at low redshift.*—The predicted redshift distribution, K counts, and angular-diameter distribution could perhaps be reproduced by a model involving a tidally triggered star formation in satellite dwarf galaxies (Lacey et al. 1993; Kauffmann et al. 1994), if the star formation activity were suitably tuned to happen near $z = 1$. However, in such models the dwarfs are accreted onto the larger of the normal galaxies by low redshifts, and few isolated remnants are expected. In contrast, our model 1 predicts between 2 and 4 galaxies per cubic megaparsec, integrated over the LF. If the galaxies expand during the supernova wind phase, as we assume, their surface brightnesses should be very low, but not beyond the detection limits of surveys currently underway, such as the drift-scan survey of Dalcanton (1995). In the *HST* F555W band (essentially V band), a rough estimate, based on the selection criteria of Dalcanton (1995), is between 12 and 25 LSB galaxies per square degree with central surface brightness $\mu_0 < 26$ mag arcsec^{-2} and exponential scale lengths greater than 3″, and between 5 and 10 galaxies per square degree with exponential scale lengths greater than 4″. It should be noted that the detection limits for the galaxies depend on both the luminosity and the surface brightness. While the luminosity estimates, which depend on the fading of the stellar populations, probably cannot be much different from what we have assumed, the surface brightness estimates are much less secure, since they depend on our assumption about the expansion of the galaxy during the supernova-wind phase.

6. *There should be an appreciable rate of Type Ia supernovae associated with the faded dwarfs.*—While there are large uncertainties in the detectability of the galaxies, if the binary star fraction is similar to that in normal galaxies, the presence of the faded boojums could be signaled Type Ia supernovae. This would be true even if the boojums exploded entirely and left behind a sea of intergalactic stars. Because the nature and evolution of the progenitors of Type Ia supernovae are uncertain (Tutukov, Yungelson, & Iben 1992; Della Valle & Livio 1994), we can make at best a rough estimate of the supernova frequency. Adopting a rate of 2.9×10^{-3} supernovae per 10^{10} $L_{\odot_B}$ from van den Bergh & Tammann (1991) and using the luminosity density for the dwarfs computed in § 4.5, there should be 9.5×10^{-6} supernovae yr^{-1} Mpc^{-3}. For a peak absolute magnitude of $B = -19.8$, this translates to 90 supernovae yr^{-1} brighter than $B = 15$ over the entire sky. This is sufficiently bright to be within the range of modern large-area surveys for transient events, but sufficiently faint that it is possible that such a rate would have escaped detection. For deeper searches, it is very likely that such isolated supernovae would have escaped detection. The recent photographic searches have all identified visible galaxies either before searching for SNe, or before carrying out spectroscopic follow-up (Hamuy 1993; Meuler 1993; Pollas 1993; McNaught 1993). The number of supernovae expected in something like the Cerro Tololo Inter-American Observatory (CTIO) search (Hamuy et al. 1993) is rather small in any case. That search identified 25 Type Ia supernovae over a period of 2 yr on roughly 1000 Schmidt plates. If the supernova rate scales with B luminosity, the number of "intergalactic" supernovae expected would be 8, even if the search had been completely unbiased with respect to visible galaxies.

6. SUMMATION

Studies of the high-redshift galaxies, of the galaxies associated with QSO absorption lines, and of the faint galaxies themselves suggest that the latter consist of two populations. The properties of the brighter of these faint galaxies (for example, those with $B \lesssim 24$) are consistent with their being the intermediate-redshift counterparts of the locally observed population of galaxies. However, the properties of the fainter galaxies are different, suggesting that at these magnitudes, the galaxy population becomes increasingly dominated by a different class of galaxies. Motivated by the large numbers of low-mass galaxies that generically arise in realistic hierarchical clustering scenarios for structure formation, various authors (e.g., Lacey & Silk 1991; Babul & Rees 1992; Gardner et al. 1993; Lacey et al. 1993; Kauffmann et al. 1994) have proposed that these very faint galaxies (boojums) are dwarf galaxies undergoing a short burst of star formation. The main difference between the various models is the mechanism(s) for triggering star formation at the appropriate epoch.

We consider the "boojums as bursting dwarfs" model of Babul & Rees (1992), which links the epoch of the formation of dwarf galaxies to the intensity of the background ionizing UV flux. This model argues that the dwarf galaxies will undergo a relatively short burst of star formation before supernova explosions expel all the gas, and that, thereafter, these galaxies will simply fade away. The bursting dwarf model has several attractive features, the three most important being (1) that the model is firmly grounded in the generally accepted hierarchical clustering scenarios for structure formation, (2) a large population of low-mass halos is a generic feature of any hierarchical model with realistic initial conditions on galactic scales, and (3) the identification of a specific mechanism (i.e., the decline in the intensity of the background UV radiation from its estimated value at $z \approx 2$) that triggers starbursts in these halos at moderate redshifts.

In and of itself, the model is difficult to analyze and compare to the observations, since it only describes the formation and evolution or dwarf galaxies. Consequently, we augment the Babul & Rees (1992) model with a phenomenological prescription for the formation and evolution of the locally observed population of galaxies (E, S0, Sab, Sbc, and Sdm types). Ideally, one would prefer a model that details the formation and evolution of all types of galaxies from initial density fluctuations. However, the pathways leading to the formation of the observed population of galaxies are neither well constrained nor well understood, whereas the star formation histories along the traditional Hubble sequence are well constrained by observations. We explore our hybrid model in detail using spectral-synthesis methods and Monte Carlo simulations of deep faint galaxy surveys. We find that for reasonable choices of star formation histories for the dwarf galaxies (the mass function and the size distribution of the dwarf galaxies are derived from realistic initial conditions for hierarchical clustering and are not ajusted to fit the data), the model results are in very good agreement with the observations. In particular:

1. The model number counts are consistent with those observed in B, I, and K bands to the faintest magnitudes surveyed. In all three bands, the dwarfs begin to dominate at $m_{AB} \sim 24$.

2. The model redshift distributions based on galaxy selection procedures that attempt to mimic the selection criteria of individual deep redshift surveys are also in good agreement with their observationally determined counterparts. Although the model predicts a large number of relatively nearby faded/fading dwarf remnants, such galaxies are difficult to detect because of their low surface brightness.

3. At the present, as well as at $z \approx 1$, the distribution of colors of the "regular" galaxies in our model is consistent with observations. Comparisons of the model color distributions of faint galaxies are also in good agreement with the observations, with colors becoming rapidly bluer in the regime dominated by the bursting dwarfs. More interestingly, though, the model does not predict an overabundance of very blue galaxies in deep K-band surveys, in spite of the fact that the dwarfs are predominantly very blue. In fact, it appears to be somewhat lacking in the blue galaxies with $K < 21$ seen by Djorgovski et al. (1995).

4. Looking back toward $z \approx 1$, the "regular" galaxies experience very modest luminosity evolution, brightening by 0.1–0.7 mag in rest-frame B_J and -0.3–0.6 mag brighter in the K band, with respect to the present.

5. At magnitudes where the model galaxy counts are dominated by the dwarf galaxies at redshifts $0.5 \lesssim z \lesssim 1$, the angular effective radii are predicted to be a few tenths of an arcsecond. Since the angular size versus redshift relation in a $q_0 = 0.5$ universe has a minimum at $z \approx 1.2$, the angular size distribution predicted by the bursting dwarf model comes close to the extreme that could be expected for any model in a spatially flat universe. Recent deep *HST* images reveal that the faint galaxies are very small; such observations favor dwarf-dominated models.

These comparisons with observations indicate that the bursting dwarf (or actually the hybrid bursting dwarf) model is a viable explanation for the puzzle of the faint galaxies. In light of recent results from gravitational lensing, angular correlation, and size distribution studies, the model may have some advantages over other competing explanations. Furthermore, as set forth in this paper, the model is amenable to specific observational tests. In particular, it predicts that (see § 5.2) number counts in the K band should continue to rise steeply at magnitudes fainter than $K_{AB} \approx 24$–25, that the redshift distribution at $B \gtrsim 25$ should be peaked at $z \lesssim 1$, and that a large population of nearby LSB dwarf galaxies should be detectable in surveys with a low isophotal detection threshold or through searches for apparently isolated Type Ia supernovae.

The bursting dwarf model is still rather schematic, due to the uncertainties in the evolution of the UV background, the density profiles of gas in minihalos, and the physics of star formation. Nevertheless, it appears to offer a promising solution to the combined problems of the counts, redshift distributions, sizes, and clustering properties of very faint galaxies.

We wish to thank Cedric Lacey, Simon Lilly, Mauro Giavalisco, Stefano Casertano, Mark Dickinson, Karl Glazebrook, and Richard Ellis for stimulating discussions and helpful suggestions. We are particularly grateful to Simon Lilly, Mark Dickinson, and Karl Glazebrook for providing us with access to their observational results prior to publication, and to Allessandro Bressan for providing us with his spectral energy distributions for comparison with our own. Finally, we wish to credit Neal Katz for coining the moniker/acronym "boojums." Support for this work is provided in part by NASA grant HF-1043, awarded by the Space Telescope Science Institute, which is operated by the Association of Universities for Research in Astronomy, Inc., for NASA under contract NAS 5-26555.

REFERENCES

Aragón-Salamanca, A., Ellis, R. S., Couch, W. J., & Carter, D. 1993, MNRAS, 262, 764
Armus, L., Heckman, T. M., Weaver, K. A., & Lehnert, M. D. 1985, ApJ, 445, 666
Babul, A., & Rees, M. J. 1992, MNRAS, 255, 346
———. 1993, in Proc. Third Teton Summer School, The Evolution of Galaxies and Their Environments (NASA CP-3190), 80
Bechtold, J., Weyman, R. J., Lin, Z., & Malkan, M. A. 1987, ApJ, 315, 180
Bertelli, G., Bressan, A., Chiosi, C., Fagotto, F., & Nasi, E. 1994, A&AS, 106, 275
Binggeli, B., Sandage, A., & Tammann, G. A. 1988, ARA&A, 26, 509
Black, J. H. 1981, MNRAS, 197, 553
Brainerd, T. G., Smail, I., & Mould, J. 1995, preprint
Bressan, A., Chiosi, C., & Fagotto, F. 1994, ApJS, 94, 63
Broadhurst, T. J., Ellis, R. S., & Glazebrook, K. 1992, Nature, 355, 55
Bruzual A., G., & Charlot, S. 1993, ApJ, 405, 538
Bruzual A., G. 1981, Ph.D. thesis, Univ. California, Berkeley
Calzetti, D., Kinney, A. L., & Storchi-Bergmann, T. 1994, ApJ, 429, 582
Charlot, S., & Bruzual A., G. 1991, ApJ, 367, 126
Charlot, S., Worthey, G., & Bressan, A. 1996, ApJ, 457, 17
Chiba, M., & Nath, B. B. 1994, ApJ, 436, 618
Clegg, R. E. S., & Middlemass, D. 1987, MNRAS, 228, 759
Colless, M. 1994, preprint
Colless, M. M., Ellis, R. S., Broadhurst, T. J., Taylor, K., & Peterson, B. A. 1993, MNRAS, 261, 19
Couch, W. J., Jurcevic, J. S., & Boyle, B. J. 1993, MNRAS, 260, 241
Cowie, L. L., Gardner, J. P., Hu, E. M., Songaila, A., Hodapp, K., & Wainscoat, R. J. 1994, ApJ, 434, 114
Cowie, L. L., Lilly, S. J., Gardner, J. P., & McLean, I. S. 1988, ApJ, 332, L29
Cowie, L. L., Songaila, A., & Hu, E. M. 1991, Nature, 354, 460
Cowie, L. L., Songaila, A., Kim, T.-S., & Hu, E. M. 1995, AJ, 109, 1522
Dalcanton, J. D. 1995, in preparation
Dalcanton, J. D. 1993, ApJ, 415, L87
Dekel, A., & Silk, J. 1986, ApJ, 303, 39
Della Valle, M., & Livio, M. 1994, 423, L31
De Propris, R., Pritchet, C. J., Harris, W. E., & McClure, R. D. 1995, ApJ, 450, 534
Dickinson, M. 1995, Ph.D. thesis, Univ. California, Berkeley
Djorgovski, S., et al. 1995, ApJ, 438, L13
Eder, J., Schombert, J. M., Dekel, A., & Oemler, A. 1989, ApJ, 340, 29
Efstathiou, G. 1992, MNRAS, 256, 43P
———. 1995, MNRAS, 272, L25
Efstathiou, G., Bernstein, G., Tyson, J. A., Katz, N., & Guhathakurta, P. 1991, ApJ, 380, L47
Ferguson, H. C., Giavalisco, M., & Babul, A. 1995, in preparation
Ferguson, H. C., & McGaugh, S. S. 1995, ApJ, 440, 470
Ferguson, H. C., & Sandage, A. 1991, AJ, 101, 765
Gardner, J. P., Cowie, L. L., & Wainscoat, R. J. 1993, ApJ, 415, L9
Glazebrook, K., Ellis, R., Colless, M., Broadhurst, T., Allington-Smith, J., & Tanvir, N. 1995, MNRAS, 273, 157
Griffiths, R., et al. 1995, in IAU Symp. 168, Examining the Big Bang and Diffuse Background Radiations (Dordrecht: Kluwer), in press
Gronwall, C., & Koo, D. C. 1995, ApJ, 440, L1
Guhathakurta, P., Tyson, J. A., & Majewski, S. R. 1990, ApJ, 359, L9
Guiderdoni, B., & Rocca-Volmerage, B. 1990, A&A, 227, 362
———. 1991, A&A, 252, 435
Hamuy, M. 1993, private communication
Hamuy, M., et al. 1993, AJ, 106, 2394
Ikeuchi, S. 1986, Ap&SS, 118, 509
Ikeuchi, S., Murakami, I., & Rees, M. J. 1989, MNRAS, 236, 21P
Im, M., Casertano, S., Griffiths, R. E., & Ratnatunga, K. U. 1995, ApJ, 441, 494
Infante, L., & Pritchet, C. J. 1995, ApJ, 439, 565
Kang, H., Shapiro, P. R., Fall, M., & Rees, M. J. 1990, ApJ, 363, 488
Kauffmann, G. 1995, preprint
Kauffmann, G., Guiderdoni, B., & White, S. D. M. 1994, MNRAS, 267, 981
Kauffmann, G., White, S. D. M., & Guiderdoni, B. 1993, MNRAS, 264, 201
Kneib, J.-P., Mathez, G., Fort, B., Mellier, Y., Soucail, G., & Langaretti, P.-Y. 1994, A&A, 286, 701
Koo, D. 1986, ApJ, 311, 651
———. 1990, in ASP Conf. Ser. 10, The Evolution of the Universe of Galaxies, ed. R. G. Kron (San Francisco: ASP), 268
Koo, D. C., & Kron, R. G. 1992, ARA&A, 30, 613
Kurucz, R. L. 1992, private communication
Lacey, C., & Cole, S. 1993, MNRAS, 262, 627
———. 1994, MNRAS, 271, 676
Lacey, C., Guiderdoni, B., Rocca-Volmerange, B., & Silk, J. 1993, ApJ, 402, 15
Lacey, C., & Silk, J. 1991, ApJ, 381, 14
Larson, R. B. 1974, MNRAS, 169, 229

Lilly, S. J. 1993, ApJ, 411, 502
Lilly, S. J., Cowie, L. L., & Gardner, J. P. 1991, ApJ, 369, 79
Lilly, S. J., Le Fevre, O., Hammer, F., Crampton, D., & Tresse, L. 1995, in Proc. 35th Herstmonceux Conf., Wide Field Spectroscopy and the Distant Universe, ed. S. J. Maddox & A. Aragón-Salamanca (Singapore: World Scientific), 281
Loveday, J., Peterson, B. A., Efstathiou, G., & Maddox, S. 1992, ApJ, 390, 338
Marlowe, A. T., Heckman, T. M., Wyse, R. F. G., & Schommer, R. 1995, ApJ, 438, 563
Marzke, R. O., Huchra, J. P., & Geller, M. J. 1994, ApJ, 428, 43
Matthews, W. 1972, ApJ, 174, 108
McNaught, R. 1993, private communication
Meuler, J. 1993, private communication
Meurer, G. R., Freeman, K. C., Dopita, M. A., & Cacciari, C. 1992, AJ, 103, 60
Mobasher, B., Ellis, R. S., & Sharples, R. M. 1986, MNRAS, 223, 11
Moore, B. 1994, Nature, 370, 629
Murakami, I., & Ikeuchi, S. 1990, PASJ, 42, L11
Mutz, S. B., et al. 1994, ApJ, 434, L55
Navarro, J. F., Frenk, C. S., & White, S. D. M. 1994, MNRAS, 267, P1
Neuschaefer, L. W., Windhorst, R. A., & Dressler, A. 1991, ApJ, 382, 32
Oke, J. B. 1974, ApJS, 27, 21
Pollas, C. 1993, private communication
Press, W. H., & Schechter, P. L. 1974, ApJ, 187, 425
Rakos, K., & Schombert, J. M. 1995, ApJ, 439, 47
Rees, M. J. 1986, MNRAS, 218, 25P
Roche, N., Shanks, T., Metcalfe, N., & Fong, R. 1993, MNRAS, 263, 360
Sandage, A. 1961, ApJ, 133, 355
Sandage, A., & Perelmuter, J.-M. 1990, ApJ, 361, 1
Schaller, G., Schaerer, D., Meynet, G., & Maeder, A. 1992, A&AS, 96, 269
Schechter, P. 1976, ApJ, 203, 297
Searle, L., Sargent, W. L. W., & Bagnuolo, W. 1973, ApJ, 179, 427
Shapiro, P. R., & Kang, H. 1987, ApJ, 318, 32
Shu, F. H. 1977, ApJ, 214, 488
Simien, F., & de Vaucouleurs, G. 1986, ApJ, 302, 564
Smail, I., Ellis, R. S., & Fitchett, M. J. 1994, MNRAS, 270, 245
Songaila, A., Cowie, L. L., Hu, E. M., & Gardner, J. P. 1994, ApJS, 94, 461
Steidel, C., & Dickinson, M. 1994, preprint
———. 1995, preprint
Steidel, C., Dickinson, M., & Persson, E. 1994, ApJ, 437, L75
Storchi-Bergmann, T., Calzetti, D., & Kinney, A. L. 1994, ApJ, 429, 572
Tinsley, B. M. 1978, ApJ, 220, 816
———. 1980, ApJ, 241, 41
Tosi, M. 1993, in ESO/OHP Workshop on Dwarf Galaxies, ed. G. Meylan & P. Prugniel (Garching: ESO), 465
Tóth, G., & Ostriker, J. P. 1992, ApJ, 389, 5
Tutukov, A. V., Yungelson, L. R., & Iben, I., Jr. 1992, ApJ, 386, 197
Tyson, J. A. 1988, AJ, 96, 1
Tytler, D. 1995, in ESO Workshop: QSO Absorption Lines, ed. G. Meylan (Garching: ESO)
van den Bergh, S., & Tammann, G. A. 1991, ARA&A, 29, 363
Wang, B. 1991, ApJ, 383, L37
White, S. D. M., & Frenk, C. S. 1991, ApJ, 379, 52
White, S. D. M., & Rees, M. J. 1978, MNRAS, 183, 341
Yoshii, Y., & Peterson, B. A. 1995, ApJ, 444, 15
Yoshii, Y., & Takahara, F. 1988, ApJ, 326, 1
Zuo, L., & Phinney, E. S. 1993, ApJ, 418, 28